Annihilation of Aromatic Cation Radicals by Ion-Pair and Radical-Pair Collapse. Unusual Solvent and Salt Effects in the Competition for Aromatic Substitution

S. Sankararaman, W. A. Haney, and J. K. Kochi*

Contribution from the Department of Chemistry, University of Houston, University Park, Houston, Texas 77004. *Received April 10, 1987*

Abstract: Aromatic cation radicals $ArH^{\bullet+}$ are spontaneously produced as solvent-caged species together with anions and radicals by the irradiation of the charge-transfer absorption band of the electron donor–acceptor complex [ArH, TNM], where ArH and TNM represent a series of anisole donors and the tetranitromethane acceptor, respectively. The subsequent fate of the geminate species [$ArH^{\bullet+}$, $C(NO_2)_3^-$, $NO_2^\bullet$] (III) depends strongly on the solvent polarity and the presence of added salts. Thus the ion-pair collapse of III to yield $ArC(NO_2)_3$ and HNO_2 is the favored process in nonpolar hydrocarbons (benzene and *n*-hexane) and in dichloromethane. On the other hand, the radical-pair collapse of III prevails in polar solvents such as acetonitrile, and it leads quantitatively to aromatic nitration ($ArNO_2$) and $HC(NO_2)_3$. The competition between ion-pair collapse and radical-pair collapse in dichloromethane is strongly affected by innocuous salts such as $Bu_4N^+ClO_4^-$ (TBAP), the presence of which leads to a dramatic change from predominantly $ArC(NO_2)_3$ to exclusively $ArNO_2$. By the same token, the common-ion salt $Bu_4N^+C(NO_2)_3^-$ (TBAT) reverses the competition, albeit less efficiently. The kinetics of ion-pair and radical-pair collapse are analyzed quantitatively by following the decay of the transients generated by the 25-ps laser-pulse excitation of the EDA complexes in various solvents and in the presence of added salts. The decay profile for ion-pair collapse to $ArC(NO_2)_3$ accords with the Winstein formulation of ion-pair equilibria as modulated by the "special salt" and "common-ion" effects with TBAP and TBAT, respectively. The residual radical-pair collapse to $ArNO_2$ follows the ion-pair separation. The observation of first-order decay kinetics with the reactive cation radicals derived from 4-haloanisoles favors geminate combination of the radical-pair [$ArH^{\bullet+}$, $NO_2^\bullet$]. The stability of the cation radical $ArH^{\bullet+}$ (as measured by the oxidation potential E° of the arene) is an important factor in the kinetics of ion-pair collapse and, to a lesser degree, in radical-pair collapse. The analyses of the aromatic isomer distributions point to the similarity in the regiospecificity for ion-pair and radical-pair collapse.

Aromatic compounds ArH are excellent electron donors, and the formation of arene cation radicals $ArH^{\bullet+}$ can occur by electron detachment at relatively low ionization energies.[1] Cation radicals from electron-rich arenes are sufficiently persistent to allow their physical properties to be examined in detail.[2] On the other hand, $ArH^{\bullet+}$ from other less endowed arenes can be quite transient, which limits their study to more indirect methods, especially with regard to their reactivity.[3,4] Among these properties, the ambivalent character of the delocalized paramagnetic ion is of particular interest since its cationic charge offers Coulombic attraction for anions ($A:^-$), whereas its unpaired electron promotes homolytic reactions with free radicals ($R^\bullet$).[5] Both the ion-pair and radical-pair interactions can lead to aromatic substitution when they collapse at a nuclear position; e.g.

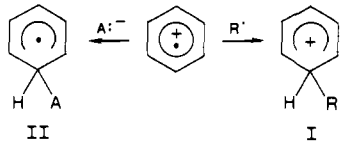

(1)

Thus the cationic adduct I represents the Wheland intermediate in electrophilic aromatic substitution,[6] and the radical adduct II is the cyclohexadienyl intermediate relevant to homolytic aromatic substitution.[7]

The competition between the ion-pair and the radical-pair annihilation as described in eq 1 can be examined directly by the charge-transfer photochemistry of electron donor–acceptor complexes. For example, it has been demonstrated that the actinic irradiation of the charge-transfer (CT) bands of arene complexes with tetranitromethane leads spontaneously to the solvent-caged triad III in eq 2.[8] Furthermore, the availability of laser-flash

$$[ArH, C(NO_2)_4] \xrightarrow{h\nu_{CT}} \underset{III}{[ArH^{\bullet+}, C(NO_2)_3^-, NO_2^\bullet]} \quad (2)$$

photolytic techniques provides the means to observe directly the kinetic behavior of III as it evolves to the products of aromatic substitution by annihilation with anions and radicals according to eq 1 for $A:^- = C(NO_2)_3^-$ and $R^\bullet = NO_2^\bullet$, respectively. Indeed, we recently showed that the collapse of the persistent cation radicals $ArH^{\bullet+}$ from various dialkoxybenzenes with $NO_2^\bullet$ leads to aromatic nitration via the Wheland intermediate.[9] The studies in this report are deliberately restricted to arenes derived from a series of monosubstituted anisoles since (a) these arene cation radicals are significantly more reactive than those derived from dialkoxybenzenes and thus (b) aromatic trinitromethylation and nitration by ion-pair and radical-pair collapse, respectively, are *competitive processes*. Such aromatic substitutions effected by charge-transfer excitation will be generically referred to hereafter as CT substitution, which is to be compared with the more conventional thermal processes leading to electrophilic and homolytic aromatic substitutions.

Results

A series of substituted arenes were examined to probe for electronic and steric effects in CT substitution, namely, anisole, the isomeric *o*-, *m*-, and *p*-methylanisoles, and the 4-substituted fluoro-, chloro-, and bromoanisoles. Each of these classes of arenes showed distinctive behavior toward aromatic substitution, and their charge-transfer photochemistry is described individually below.

(1) (a) Kobayashi, T.; Nagakura, S. *Bull. Chem. Soc. Jpn.* **1974**, *47*, 2563. (b) For a recent summary and leading references, see: Howell, J. O.; Goncalves, J. M.; Amatore, C.; Klasinc, L.; Wightman, R. M.; Kochi, J. K. *J. Am. Chem. Soc.* **1984**, *106*, 3968.

(2) Kaiser, E. T.; Kevan, L., Eds. *Radial Ions*; Wiley: New York, 1968.

(3) Yoshida, K. *Electrooxidation in Organic Chemistry*; Wiley: New York, 1984.

(4) Bard, A. J.; Ledwith, A.; Shine, H. J. *Adv. Phys. Org. Chem.* **1976**, *14*, 155.

(5) For a recent review of nucleophilic addition to aromatic cation radicals, see ref 3. The corresponding homolytic addition to aromatic cation radicals has not been examined heretofore.

(6) (a) Wheland, G. W. *J. Am. Chem. Soc.* **1942**, *64*, 900. (b) Ingold, C. K. *Structure and Mechanism in Organic Chemistry*, 2nd ed.; Cornell University Press: Ithaca, NY, 1969.

(7) Perkins, M. J. In *Free Radicals*; Kochi, J. K., Ed.; Wiley: New York, 1973; Vol. 2, p 231ff.

(8) Masnovi, J. M.; Kochi, J. K.; Hilinski, E. F.; Rentzepis, P. M. *J. Am. Chem. Soc.* **1986**, *108*, 1126.

(9) Sankararaman, S.; Haney, W. A.; Kochi, J. K. *J. Am. Chem. Soc.* **1987**, *109*, 5235.

0002-7863/87/1509-7824$01.50/0

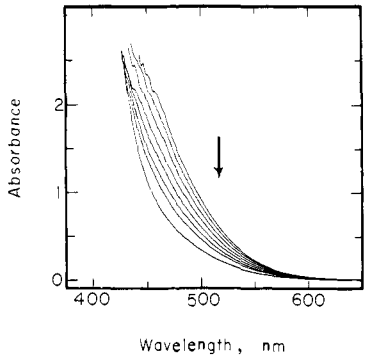

Figure 1. Typical bleaching of the CT absorption band upon constant irradiation at $\lambda > 425$ nm as shown for 0.10 M 4-methylanisole and 0.8 M TNM in dichloromethane after (top to bottom) 0, 10, 20, 30, 40, 50, and 70 min at 25 °C.

I. Charge-Transfer Substitutions of Arenes with Tetranitromethane. Products and Stoichiometry. The behavior of *p*-methylanisole exemplifies the strikingly dichotomous aromatic substitutions that are available simply by a change of solvent in which the CT photochemistry of arenes with tetranitromethane (TNM) was carried out.

A. Aromatic Alkylation. In **dichloromethane**, the light orange solution of 0.1 M *p*-methylanisole containing 0.8 M tetranitromethane gradually bleached upon exposure to visible light ($\lambda >$ 425 nm) at 25 °C, as shown by the spectral changes in Figure 1. An inspection of the ^{1}H NMR spectrum of the reaction mixture indicated the complete disappearance of the pair of characteristic methyl resonances of *p*-methylanisole at δ 2.28 and 3.75, and they were replaced by a new pair of singlets at δ 2.35 and 3.80. The aromatic product was isolated as yellow crystals in 90% yield, and it was identified as 4-methyl-2-(trinitromethyl)anisole (see Experimental Section) after removal of the volatiles in vacuo and crystallization of the red-brown slurry from an ether–hexane mixture.[10] The amount of accompanying nitrous acid was determined volumetrically by treatment of the reaction mixture with urea.[11] Accordingly, the stoichiometry in eq 3 represents the introduction of the trinitromethyl moiety cleanly into the aromatic ring with an accompanying transfer of the hydrogen to NO_2. Such a transformation is tantamount to aromatic nitroalkylation, and the generic process will be referred to hereafter simply as *alkylation*.[12]

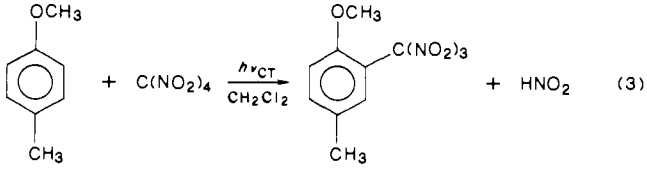

B. Aromatic Nitration. In **acetonitrile**, a solution of 0.1 M *p*-methylanisole containing 0.8 M tetranitromethane underwent a color change similar to that shown in Figure 1 when exposed to visible light ($\lambda > 425$ nm) at 25 °C. However, inspection of the ^{1}H NMR spectrum of the reaction mixture quickly revealed that another aromatic product was formed with a pair of methyl resonances at δ 3.95 (3 H) and 2.35 (3 H). Subsequent isolation and spectral comparison with an authenic sample indicated that 4-methyl-2-nitroanisole[13] was formed in virtually quantitative yields when the CT photochemistry was carried out under rigorously anhydrous conditions. The accompanying trinitromethyl moiety was identified as nitroform by extraction of the crude reaction mixture (after dilution by ether) with water. The subsequent spectrophotometric analysis of the aqueous extract showed that 1 equiv of nitroform[14] was formed according to the stoichiometry in eq 4. Under these conditions there was no contamination by the product of trinitromethylation.[16] The stoichiometry in eq 4 represents the introduction of a nitro group cleanly into the aromatic ring with an accompanying proton transfer to the trinitromethide ion. As such, this CT substitution will be referred to hereafter simply as *nitration*.

Table I. Charge-Transfer Nitration of Anisole and Derivatives in Acetonitrile Solutions[a]

aromatic donor	yield,[b] %			
	2-NO_2	3-NO_2	4-NO_2	others
anisole	35	3	43	
2-methylanisole			68	6-NO_2 (32)
3-methylanisole	16		54	6-NO_2 (30)
4-methylanisole	60			2-nitro-4-methylphenol (40)
4-fluoroanisole	83			2,6-dinitro-4-fluorophenol (14)
4-chloroanisole	100			
4-bromoanisole	42			4-nitroanisole (38) 2,4-dibromoanisole (20)

[a] By CT excitation of the EDA complexes from 0.10 M anisoles and 0.8 M TNM at $\lambda > 425$ nm at 25 °C. [b] Yields based on stoichiometry in eq 4.

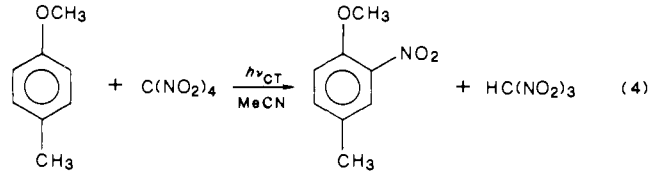

C. In hydrocarbons such as *n*-hexane and benzene, the CT substitution of *p*-methylanisole with tetranitromethane afforded a mixture of products derived from both alkylation (eq 3) and nitration (eq 4). Thus the CT irradiation of 0.06 M *p*-methylanisole in hexane containing 0.3 M tetranitromethane yielded 4-methyl-2-(trinitromethyl)anisole and 4-methyl-2-nitroanisole in 85% and 15% yields, respectively. A similar mixture was obtained when benzene was employed as the solvent.

II. Solvent Effect in the Competition for CT Nitration and Alkylation. Owing to the distinctive stoichiometries observed in dichloromethane (eq 3) and in acetonitrile (eq 4), we examined the generality of the solvent effect by exposing the isomeric *o*- and *m*-methylanisoles as well as the parent anisole and the *p*-haloanisoles to CT substitution in both of these solvents.

Aromatic Nitration. The various aromatic products and yields obtained by the CT irradiation of the aromatic complexes with tetranitromethane in acetonitrile are summarized in Table I. In every case, the quantitative yields of nitroform in the reaction mixture indicated that the stoichiometry in eq 4 applied. Among the products of aromatic nitration, the isomer distributions pointed to a strong preference for the substitutions to occur at positions ortho and para to the methoxy group. In addition, a series of characteristic byproducts from aromatic nitration were observed. For example, the identification of *p*-nitroanisole and 2,4-dibromoanisole from 4-bromoanisole was highly diagnostic of an (electrophilic) nitrodebromination by ipso substitution at the para position.[17,18] Control experiments showed that the dinitration of *p*-fluorophenol could have arisen from the further CT substitution of the first-formed 4-fluoro-2-nitrophenol as a result of

(10) A small amount (5%) of 4-methyl-2-nitroanisole was also formed.
(11) Clowes, F.; Coleman, J. B. *Quantitative Chemical Analysis*, 5th ed.; Blakiston's and Sons: London, 1900; p 495.
(12) For a homolytic process for aromatic nitroalkylation, see: Kurz, M. E.; Chen, R. T. Y. *J. Org. Chem.* **1978**, *43*, 239.
(13) Vouros, P.; Petersen, B.; Dafeldecker, W. P.; Neumeyer, J. L. *J. Org. Chem.* **1977**, *42*, 744.
(14) By spectral analysis of trinitromethide ($\lambda_{max} = 350$ nm, $\epsilon_{max} = 14000$ M^{-1} cm^{-1}) from the acid dissociation of nitroform.[15]
(15) Masnovi, J. M.; Kochi, J. K. *J. Am. Chem. Soc.* **1985**, *107*, 7880.
(16) For the accompanying nitrophenols from the demethylation of the methoxy group from traces of water in acetonitrile, see Table I and eq 5 and 6.
(17) Perrin, C. L.; Skinner, G. A. *J. Am. Chem. Soc.* **1971**, *93*, 3389.
(18) (a) Bunton, C. A.; Hughes, E. O.; Ingold, C. K.; Jacobs, D. J. H.; Jones, M. H.; Minkoff, G. J.; Reed, R. I. *J. Chem. Soc.* **1950**, 2628. (b) Reverdin, F.; During, F. *Chem. Ber.* **1899**, *32*, 152. (c) Robinson, G. M. *J. Chem. Soc.* **1916**, *109*, 1078.

Table II. Charge-Transfer Trinitromethylation of Anisole and Its Derivatives in Dichloromethane[a]

aromatic donor	yield,[b] % 2-$C(NO_2)_3$	other products	material balance
anisole	40[c]	2-nitroanisole (22) 4-nitroanisole (28)	90
2-methylanisole	60[d]	2-methyl-4-nitroanisole (10) 2-methyl-6-nitroanisole (6)	80
3-methylanisole	62[e]	3-methylnitroanisoles[f]	
4-methylanisole	95	4-methyl-2-nitroanisole (5)	100
4-fluoroanisole	72	4-fluoro-2-nitroanisole (9) 4-fluoro-2,6-dinitroanisole (6)	87
4-chloroanisole	67	4-chloro-2-nitroanisole (7)	74
4-bromoanisole	73	4-bromo-2-nitroanisole (7) 4-nitroanisole (6) 2,4-dibromoanisole (5)	91

[a] See Table I for conditions. [b] Yields based on stoichiometry in eq 3. [c] 4-(Trinitromethyl)anisole. [d] 2-Methyl-4-(trinitromethyl)anisole. [e] 3-Methyl-4-(trinitromethyl)anisole. [f] Mixture of 2-, 4-, and 6-nitro-3-methylanisoles.

the prolonged irradiation required to effect the complete conversion of *p*-fluoroanisole. The phenolic product derived from the demethylation of the methoxy group in *p*-fluoroanisole occurred during CT substitution, since the nitrated anisole was stable to reaction conditions. Furthermore, the demethylation of the methoxy group was most likely to occur when care was not exercised to remove adventitious water from the acetonitrile solvent. Thus the CT substitution of 4-methylanisole with TNM in acetonitrile, in the absence of extra precautions to remove water, yielded 4-methyl-2-nitroanisole (60%) and significant amounts (40%) of 4-methyl-2-nitrophenol. The repetition of this experiment at 0 °C revealed the presence of a transient new species, which was identified as 6-methyl-6-nitrocyclohexa-2,5-dienone from its characteristic ^1H NMR spectrum.[19] The solution upon standing at room temperature was completely converted to 4-methyl-2-nitrophenol,[20] i.e.

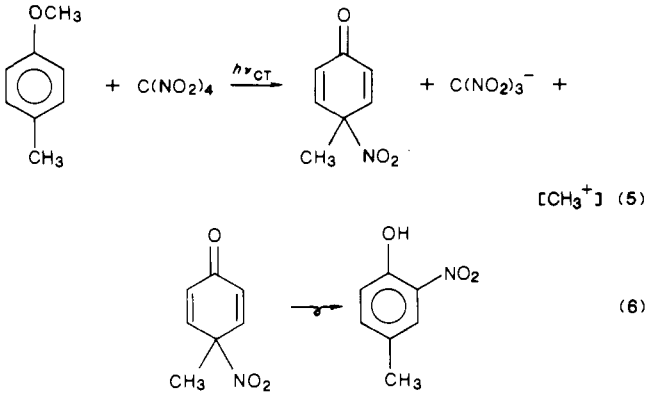

Aromatic Alkylation. The various aromatic products and yields obtained by the CT irradiation (at $\lambda > 425$ nm) of the aromatic complexes with tetranitromethane in dichloromethane are summarized in Table II. In each case, the principal product was derived from the introduction of a single trinitromethyl group into the aromatic ring to accord with the stoichiometry in eq 3. The positional isomers were determined by the acidic hydrolysis to the corresponding carboxylic acid,[21] i.e.

$$ArC(NO_2)_3 + H_2O \xrightarrow{[H^+]} ArCO_2H, \text{ etc.} \quad (7)$$

followed by comparison with authentic samples of $ArCO_2H$, as described in the Experimental Section. Only one isomer was obtained, and it arose from alkylation at a position either ortho or para to the methoxy group. Otherwise the relatively minor amounts of nitration byproducts corresponded to those obtained in acetonitrile (compare with the results in Table I).

III. Salt Effects on the Competition for CT Nitration and Alkylation. The solvent-induced competition between CT alkylation and nitration as sharply delineated in eq 3 and 4, respectively, has its exact counterpart in the marked salt effects shown in Table III. The influence of salt on CT substitution was examined with two types, in which the innocuous cation tetra-*n*-butylammonium (TBA) was paired with either the common anion $C(NO_2)_3^-$ (T, i.e., as TBAT) or the innocuous anion ClO_4^- (P, i.e., as TBAP).[15,22]

The most dramatic influence of salt was observed in the complete reversal of the product distribution in dichloromethane. Thus entries 1–3 in Table III show that predominance of alkylation in this solvent (see eq 3) was negated by the presence of the innocuous salt TBAP and totally replaced with nitration; i.e.

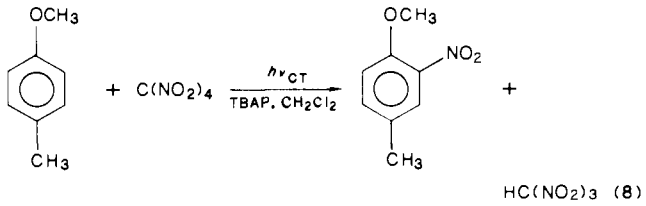

Furthermore, the presence of the common-ion salt TBAT even in small amounts (0.01 M)[23] promoted nitration at the expense of alkylation (compare entries 1 and 4, Table III). It is important to emphasize that such a salt effect ran counter to the increased availability of trinitromethide during the CT substitution.

The salt effects were significantly less pronounced in highly nonpolar solvents such as benzene. Thus the presence of 0.01 M TBAP had only a minor effect on decreasing alkylation from 85% to only 75% (see entries 9 and 10). Conversely, the presence of 0.01 M common-ion salt TBAT was sufficient to wipe out the small amount (15%) of nitration completely (entry 11).

At the other end of solvent polarity, the salt effects were also minor in acetonitrile. Thus the small amount (5%) of alkylation (entry 5) was increased slightly to 10% by the presence of the common-ion salt TBAT. It was completely wiped out by the innocuous salt TBAP (entry 6, Table III).

IV. Quantum Yields for Charge-Transfer Substitution. The photoefficiencies of the charge-transfer alkylation (eq 3) and nitration (eq 4) of 4-methylanisole were measured with a Reinecke actinometer[24] and carried out with monochromatic light by passing the output from a 500-W high-pressure mercury lamp through a 520-nm interference filter (10-nm band-pass). The quantum yields for the formation of 4-methyl-2-(trinitromethyl)anisole and 4-methyl-2-nitroanisole were obtained from individual photolysis runs. The formation of 4-methyl-2-(trinitromethyl)anisole was quantitatively analyzed by separation on a C-18 reverse-phase column with high-pressure liquid chromatography (HPLC) and quantified with UV detection. A calibration curve was based on the integrated chromatographic peak as a function of the concentration of pure 4-methyl-2-(trinitromethyl)anisole. The formation of 4-methyl-2-nitroanisole was quantified by HPLC analysis using a column consisting of silica gel. The quantum yield for the disappearance of the arene was determined by the liquid chromatographic analysis of 4-methylanisole before and after irradiation. Owing to the experimental difficulty in the HPLC analysis of small amounts of substitution products accrued over long irradiation times (see Table IV), the quantum yields are to be considered reliable to one significant figure.[25]

(19) Barnes, C. E.; Feldman, K. S.; Johnson, M. W.; Lee, H. W. H.; Myhre, P. C. *J. Org. Chem.* **1979**, *44*, 3925.
(20) (a) Barnes, C. E.; Myhre, P. C. *J. Am. Chem. Soc.* **1978**, *100*, 973. (b) The loss of methyl in eq 5 (and eq 26) can occur from the σ-adduct I by direct transfer to water or more likely by addition of water followed by elimination of methanol and deprotonation. These pathways can be distinguished by isotopic labeling with water-^{18}O and analysis of the methanol.
(21) Kamlet, M. J.; Kaplan, L. A.; Dacons, J. C. *J. Org. Chem.* **1961**, *26*, 4371.
(22) Innocuous ions are not included among the aromatic products.
(23) The amounts of TBAT that could be added were limited by its intense absorption (see ref 15.)
(24) Wegner, E. E.; Adamson, A. W. *J. Am. Chem. Soc.* **1966**, *88*, 394.

Table III. Salt Effects on Charge-Transfer Substitutions[a]

solvent	ArH,[b] M	TNM, M	salt[c]	time,[d] h	products,[e] % 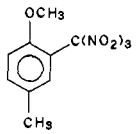	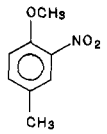	isolated yield[f]
CH_2Cl_2	0.06	0.66		5	95	5	70
CH_2Cl_2	0.06	0.83	TBAP (0.2 M)	5	0	100[g]	
CH_2Cl_2	0.10	0.55	TBAP (0.01 M)	6	0	100[h]	
CH_2Cl_2	0.06	2.22	TBAT (0.01 M)	6.5	76	24	
MeCN	0.06	1.67		6.5	5	95[i,l]	
MeCN	0.13	1.39	TBAP (0.2 M)	6	0	100[j,m]	
MeCN	0.06	1.39	TBAT (0.01 M)[n]	7	10	90[k]	
n-C_6H_{14}	0.06	0.28		5	85	15	70
C_6H_6	0.03	0.55		5	85	15	72
C_6H_6	0.06	0.55	TBAP (0.01 M)[o]	3.5	75	25	
C_6H_6	0.06	1.50	TBAT (0.01 M)[o]	6.5	100	0	

[a] From CT irradiation of 3 mL of solution with $\lambda > 425$ nm. [b] 4-Methylanisole. [c] Tetra-n-butylammonium trinitromethide (TBAT) and perchlorate (TBAP). [d] Duration of irradiation. [e] Based on ^{1}H NMR analysis with either nitromethane or dichloromethane as internal standard, unless indicated otherwise. [f] Of major product by crystallization. [g-k] Includes 4-methyl-2-nitrophenol in 35%,[g] 39%,[h] 14%,[i] 6%,[j] and 13%[k] yield. [l,m] Includes 4-methyl-2,6-dinitrophenol in 15%[l] and 39%[m] yield. [n] Irradiation with $\lambda > 480$ nm. [o] Saturated solution.

Table IV. Quantum Yields for Charge-Transfer Substitutions[a]

arene,[b] M	TNM, M	solvent	salt[c]	time,[c] h	$\Phi^d_{C(NO_2)_3}$	$\Phi^e_{NO_2}$	$-\Phi^f_{Ar}$
0.2	1.17	CH_2Cl_2		8	0.19		
0.2	1.17	CH_2Cl_2	TBAT (0.1 M)	7	0.17		
0.2	1.17	CH_2Cl_2	TBAP (0.2 M)	7	*g*		
0.2	1.17	CH_2Cl_2	TBAP (0.2 M)	12		0.13	
0.2	1.17	CH_2Cl_2		8			0.24
0.2	1.5	MeCN		8	0.02		
0.2	1.5	MeCN	TBAT (0.01 M)	8	0.05		
0.2	1.5	MeCN	TBAP (0.2 M)	8	*h*		
0.2	1.5	MeCN		12		0.13	
		MeCN					0.16
0.2	0.84	n-C_6H_{14}		7	0.19		
0.2	0.84	C_6H_6		7	0.22		
0.2	0.84	C_6H_6		12	0.06		
0.2	0.84	C_6H_6	TBAT (0.01 M)	7	0.18		
0.2	0.84	C_6H_6	TBAP (0.01 M)	8	0.11		
0.2	0.84	C_6H_6	TBAP (0.01 M)	12		0.08	
0.2	1.17	C_6H_6		8			0.19

[a] From CT irradiation of 2 mL of solution at $\lambda = 520 \pm 5$ nm. [b] 4-Methylanisole. [c] See Table III. [d-f] Quantum yield for trinitromethylation,[d] nitration,[e] and arene loss.[f] [g,h] Measured as $\sim 10^{-3}$ [g] and [h] 0.005.[h]

The results summarized in Table IV show the quantum yield to be roughly 0.2 for aromatic alkylation and nitration of 4-methylanisole. The quantum yield of 0.2 for product formation was in reasonable agreement with the quantum yield measured for the disappearance of arene. The measured quantum yields for alkylation and nitration were both by and large independent of the solvent. We also judge from those measurements made when alkylation predominated that the quantum yields were also independent of salt. In the instances in which alkylation was a minor pathway, the quantum yields appeared to fall off with added salt. The latter, however, may be an experimental artifact.[25]

In order to identify the photochemical process that led to charge-transfer substitution, we turned to the spectral changes attendant upon the exposure of the various anisoles to tetranitromethane.

V. Charge-Transfer Spectra and the Formation Constants of the EDA Complexes of Anisoles with Tetranitromethane. When tetranitromethane and 4-methylanisole were mixed, an instantaneous coloration of the solution was observed which varied from wine red to deep yellow depending on the concentrations of each component and the solvent. The corresponding change in the absorption spectra is illustrated in Figure 2, together with those of the related anisoles. The colors formed upon the exposure of the various anisoles to tetranitromethane are clearly associated with the appearance of these new absorption bands (Figure 2B)

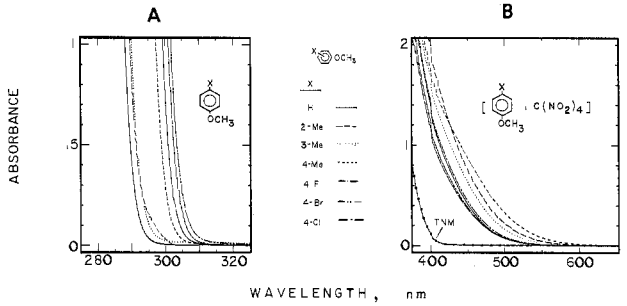

Figure 2. Absorption spectra of (A) uncomplexed anisole donors and (B) 1:1 EDA complex from 0.1 M anisole donor and 0.5 M TNM in dichloromethane as indicated.

since neither tetranitromethane nor the anisoles absorb in the visible region (Figure 2A).

The maxima of the absorption bands were obscured by the low-energy tails of the uncomplexed anisoles (Figure 2A) and tetranitromethane (Figure 2B). Nonetheless the consistent red shift of the broad tails with the more electron-rich anisoles is characteristic of charge-transfer transitions associated with intermolecular electron donor–acceptor complexes.[26,27] As con-

(25) The HPLC analysis of the alkylation product was particularly difficult at low concentrations.

(26) Mulliken, R. S.; Person, W. B. *Molecular Complexes: A Lecture and Reprint Volume*; Wiley: New York, 1969.

(27) Foster, R. *Organic Charge Transfer Complexes*; Academic: New York, 1969.

Table V. Formation Constants of the EDA Complexes of Substituted Anisoles with Tetranitromethane[a]

aromatic donor	formation constant K, M^{-1} CH_2Cl_2	MeCN	ϵ_{CT},[b] M^{-1} cm^{-1}
anisole	0.28 (0.26)	0.21 (0.21)	26 (13)
2-methylanisole	0.25 (0.26)	0.32 (0.34)	59 (33)
3-methylanisole	0.23 (0.22)		49 (27)
4-methylanisole	0.19 (0.19)	0.19 (0.20)	97 (66)
4-fluoroanisole	0.26 (0.28)[c]	0.20 (0.21)	62 (44)[c]
4-chloroanisole	0.23 (0.23)[c]		75 (56)[c]
4-bromoanisole	0.27 (0.28)[c]	0.22 (0.22)	57 (30)[c]

[a] In dichloromethane or acetonitrile containing 0.1 M arene and 0.3–1.0 M TNM at 25 °C. [b] Measured at 480 nm (values in parentheses measured at 500 nm) in CH_2Cl_2, unless indicated otherwise. [c] At 450 nm (460 nm).

sidered for the anisoles (ArH) and tetranitromethane important to CT substitution, the relevant equilibrium is

$$\mathrm{ArH} + \mathrm{C(NO_2)_4} \overset{K}{\rightleftharpoons} [\mathrm{ArH, C(NO_2)_4}] \qquad (9)$$

All of these CT bands persisted indefinitely at room temperature if the solutions were protected from adventitious exposure to room light. When these solutions were deliberately irradiated with visible light (filtered for $\lambda > 425$ nm), the monotonic decreases in the CT absorption band (compare Figure 1) were visually observed as the bleaching of the red-orange solution. We thus conclude that the EDA complexes formed in eq 9 are the important precursors responsible for charge-transfer substitution.

The amounts of the EDA complex present in solution were measured spectrophotometrically by the Benesi–Hildebrand procedure.[28,29] For the 1:1 complex in eq 9, the changes in the absorbance A_{CT} of the charge-transfer band at various concentrations of the aromatic donor and TNM are given by

$$\frac{[\mathrm{ArH}]}{A_{CT}} = \frac{1}{\epsilon_{CT}} + \frac{1}{K\epsilon_{CT}[\mathrm{TNM}]} \qquad (10)$$

under conditions in which [TNM] ≫ [ArH]. To avoid complications arising from higher order 2:1 complexes, all the spectral measurements were made with tetranitromethane in excess. Since only the absorption tails of the CT bands were observed in Figure 2B, the absorbance of the substituted anisoles was measured at two wavelengths, typically 480 and 500 nm, except the haloanisoles, which were measured at 450 and 460 nm. Each of the Benesi–Hildebrand plots consisted of at least eight data points, and the resulting linear fit was obtained by the method of least squares with a correlation coefficient >0.99. The values of the formation constant K in eq 9 and the extinction coefficient ϵ_{CT} of the various EDA complexes are included in Table V. The limited magnitudes of K indicated that the complexes of anisoles with tetranitromethane which were relevant to CT substitution be best classified as weak. More importantly, the slight change in the magnitudes of K from dichloromethane to acetonitrile was not sufficient to serve as a solvent-based differentiation of the EDA complexes.

VI. Transient Absorption Spectra of the Reactive Intermediates in Charge-Transfer Substitutions. In order to identify the reactive intermediates in the charge-transfer substitution, we examined the time-resolved spectra immediately following the application of a 25-ps laser pulse at 532 nm. Since the energy of this excitation pulse corresponded to only the tails of the CT absorption bands in Figure 2B, there was no ambiguity about either the adventitious local excitation of the uncomplexed anisole (see Figure 2A) or the generation of intermediates unrelated to the CT excitation of the EDA complexes. Furthermore, tetranitromethane was completely transparent at these wavelengths (see Figure 2B), and there was no possibility of photoinducing a homolytic cleavage[30]

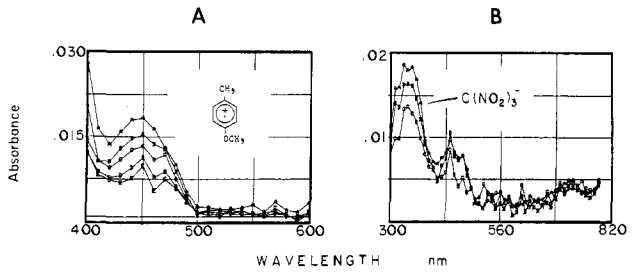

Figure 3. Transient absorption spectra derived from the CT excitation at 532 nm of the EDA complex in dichloromethane from (A) 0.1 M 4-methylanisole and 0.42 M TNM taken at 8, 26, 54, 74, and 109 μs and (B) 0.2 M 4-methylanisole and 0.02 M TNM taken at 4, 22, and 84 μs following the laser pulse.

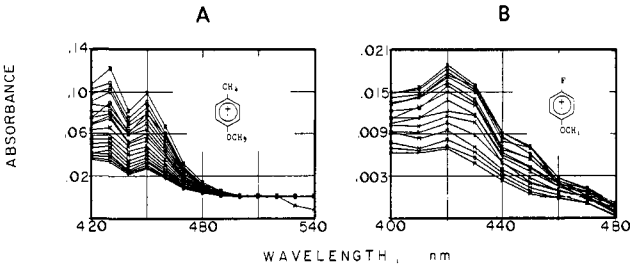

Figure 4. Spectral transients from the CT irradiation with $\lambda = 532$ nm of (A) 0.1 M 4-methylanisole and 0.8 M TNM and (B) 0.2 M 4-fluoroanisole and 0.4 M TNM in acetonitrile.

to $^{\bullet}C(NO_2)_3$ and/or $^{\bullet}NO_2$. The charge-transfer excitation of the EDA complex with the laser pulse was carried out under two conditions, namely, that relevant to (A) aromatic alkylation as described in eq 3 and (B) aromatic nitration as described in eq 4.

A. Aromatic Alkylation. The intense absorption in Figure 3A was observed in the visible region between 400 and 500 nm immediately following (<100 ns) the 532-nm laser-pulse excitation of the EDA complex from 0.1 M 4-methylanisole and 0.4 M tetranitromethane in dichloromethane. The transient absorption band with $\lambda_{max} = 450$ nm corresponded to the cation radical of 4-methylanisole by comparison with the absorption spectra of analogous species generated by pulse radiolysis.[31] Any transient absorptions below 400 nm could only be observed with solutions of the EDA complex made up with minimum amounts of the acceptor (e.g., 0.02 M tetranitromethane and 0.2 M 4-methylanisole), owing to interference from the low-energy tail of the TNM absorption (compare Figure 2B).[14] Under these conditions a second absorption band with $\lambda_{max} = 350$ was clearly visible (Figure 3B). The latter coincided with the spectrum of the trinitromethide anion, as confirmed by the spectral comparison with that of an authentic sample of $n\text{-}Bu_4N^+C(NO_2)_3^-$.[8,15] From the relative intensities of the absorption bands in Figure 3B for the aromatic cation radical and the trinitromethide anion, we conclude that they were produced concomitantly and in equimolar amounts under the reaction conditions extant in CT alkylation, i.e.

$$[\mathrm{ArH, C(NO_2)_4}] \xrightarrow[\mathrm{CH_2Cl_2}]{h\nu_{CT}} \mathrm{ArH}^{\bullet +} + \mathrm{C(NO_2)_3^-} + \mathrm{NO_2}^{\bullet} \qquad (11)$$

Nitrogen dioxide was not observed directly due to the weak and diffuse character of its absorption spectrum,[32] and the presence in eq 11 was inferred from the stoichiometry.

B. Aromatic Nitration. The transient absorption spectrum of the aromatic cation radical was also apparent (Figure 4A) from the application of the 532-nm laser pulse under the conditions extant in CT nitration, namely, 0.1 M 4-methylanisole and 0.8

(28) Benesi, H. A.; Hildebrand, J. H. *J. Am. Chem. Soc.* **1949**, *71*, 2703.
(29) (a) Person, W. B. *J. Am. Chem. Soc.* **1965**, *87*, 167. (b) Foster, R. *Molecular Complexes*; Crane, Russak and Co.: New York, 1974; Vol. 2.
(30) Altukhov, R. V.; Perekalin, V. V. *Russ. Chem. Rev.* (*Engl. Transl.*) **1976**, *45*, 1052.
(31) See: O'Neill, P. O.; Steenken, S.; Schulte-Frohlinde, D. *J. Phys. Chem.* **1975**, *79*, 2773.
(32) (a) Hall, T. C., Jr.; Blacet, F. E. *J. Chem. Phys.* **1952**, *20*, 1745. (b) Gillespie, G. D.; Khan, A. U. *J. Chem. Phys.* **1976**, *65*, 1624 and references therein.

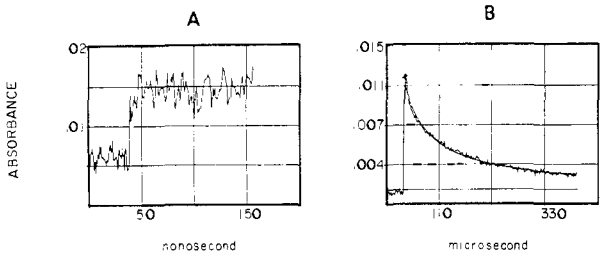

Figure 5. Decay behavior of the transient absorption at 460 nm of 4-methylanisole cation radical following the CT excitation at 532 nm of 0.1 M 4-methylanisole and 0.8 M TNM in dichloromethane with a 25-ps laser pulse. The fit of the experimental decay to second-order kinetics is shown in (B) by the fit to the smooth curve obtained from the computer-generated least-squares fit of the data.

Table VI. Decay Kinetics of the Anisole Cation Radicals for CT Trinitromethylations in Dichloromethane[a]

X-anisole		TNM,	time scale,		rate	λ,[d]
X	concn, M	M	μs	kinetics[b]	constant[c]	nm
4-methyl	0.10	0.42	10–100	2°	1.6×10^6	470
4-fluoro	0.20	0.42	10–100	2°	1.9×10^7	500
4-chloro	0.20	0.42	2–40	2°	2.0×10^7	500
4-bromo	0.20	0.42	2–20	2°	3.6×10^7	490

[a] Following the 25-ps laser pulse at 532 nm at 25 °C in dichloromethane. [b] Second-order kinetics (2°). [c] Second-order rate constant in absorbance units of A^{-1} s^{-1}. [d] Monitoring wavelength.

M tetranitromethane in acetonitrile. The slight blue shift of the absorption maximum of 4-methylanisole cation radical in acetonitrile (Figure 4A) relative to that in dichloromethane follows from the increase in solvent polarity.[33] The absorption spectrum of the cation radical derived from 4-fluoroanisole by an analogous procedure was similar (Figure 4B) to that of the methyl analogue except for a small blue shift. Indeed the substituent effect on the absorption spectrum of the haloanisole cation radicals is shown by the increasing trend of λ_{max} = 420, 454, and 500 nm for *p*-fluoro, *p*-chloro, and *p*-bromo, respectively, in acetonitrile solution. In each case the identity of the aromatic cation radical was confirmed by spectral comparison with authentic species generated by time-resolved pulse radiolysis (see Experimental Section).

VII. Solvent Effects on the Decay Kinetics for Aromatic Cation Radicals during CT Substitutions. The transitory character of the various aromatic cation radicals following their spontaneous production by laser excitation was quantitatively assessed by measuring the temporal decrease of the absorbances under conditions that were clearly relevant to CT alkylation (eq 3) and nitration (eq 4). Indeed the lifetimes of the cation radicals were highly dependent on the solvent. For example, in hexane, the cation radical from 4-methylanisole persisted only up to ~50 ns, whereas in acetonitrile it was visible to beyond 400 ns.

Owing to their unique patterns of decay, the various anisole cation radicals will be discussed separately in (A) dichloromethane, (B) acetonitrile, and (C) *n*-hexane.

A. In dichloromethane, the laser-pulse excitation of the 4-methylanisole/TNM complex led to an instantaneous rise in the 470-nm absorbance of the cation radical as shown in Figure 5A. This was followed by a short period of relative quiescence on the nanosecond time scale; finally the slower decay on the microsecond time scale is shown in Figure 5B. The clean adherence to second-order kinetics is indicated by the excellent fit to the smooth curve drawn in Figure 5B from the computer-fitted least-squares treatment of the decay profile.[34] The second-order rate constant

(33) (a) Dimroth, K.; Reichardt, C.; Siepman, T.; Bohlmann, J. *Liebigs Ann. Chem.* **1963**, *661*, 1. (b) Reichardt, C. *Angew. Chem., Int. Ed. Engl.* **1965**, *4*, 29. (c) Kosower, E. M. *Introduction to Physical Organic Chemistry*; Wiley: New York, 1968; p 293ff.

(34) (a) The computer-generated decay curves were based on the initial and the final absorbances indicated with asterisks in the figures. (b) The kinetics order was always derived from extensive trials and represented unambiguous fits to the experimental decay (with the exceptions noted).

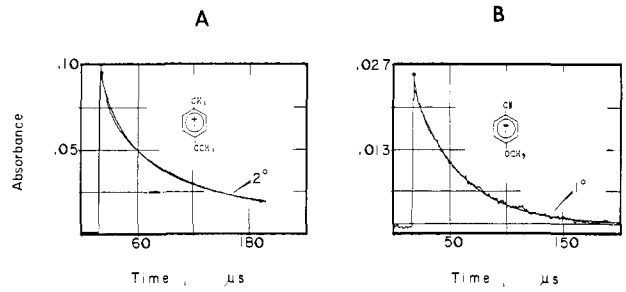

Figure 6. Second-order and first-order rate of disappearance of the cation radical from (A) 4-methylanisole and (B) 4-chloroanisole, respectively, as derived by CT excitation of the EDA complex from 0.2 M donor and 0.4 M TNM in acetonitrile as in Figure 5.

Table VII. Decay Kinetics of the Anisole Cation Radicals for CT Nitrations in Acetonitrile[a]

X-anisole		TNM,	time scale,		rate	λ,[d]
X	concn, M	M	μs	kinetics[b]	constant[c]	nm
4-methyl	0.10	0.84	10–200	2°	2.5×10^5	450
4-fluoro	0.20	1.2	10–100	1°	1.9×10^4	450
4-chloro	0.20	1.2	20–200	1°	2.4×10^4	450
4-bromo	0.20	1.2	10–100	1°	3.7×10^4	500

[a] Following the 25-ps laser pulse at 532 nm at 25 °C in acetonitrile. [b] Second-order (2°) and first-order (1°) kinetics. [c] Second-order rate constant (k_2) in absorbance units of A^{-1} s^{-1} and first-order rate constant (k_1) in s^{-1}. [d] Monitoring wavelength.

$k_2 = 1.6 \times 10^6$ A^{-1} s^{-1} in absorbance units (Table VI) was applicable to the complete disappearance of the cation radical. The residual absorbance at this wavelength was tentatively attributed to the broad absorption of the unreacted NO_2.[35] Moreover, the second-order rate constant, which was essentially unaltered by changes in the intensity of the laser pulse, confirmed this kinetics analysis.

The disappearance of the cation radicals of the 4-haloanisoles followed the same decay pattern. The second-order rate constants obtained in dichloromethane are summarized in Table VI. The results show that all the anisole cation radicals followed the same decay pattern in dichloromethane with second-order rate constants that were not highly distinguished from one another.[36]

B. In acetonitrile under conditions in which CT nitration prevailed, the kinetics behavior of each anisole cation radical was different. For example, Figure 6A shows that the decay of the 4-methylanisole cation radical in acetonitrile followed second-order kinetics with the rate constant $k_2 = 2.5 \times 10^5$ A^{-1} s^{-1} (Table VII). On the other hand, the cation radicals of the 4-haloanisoles formed by the same CT excitation consistently followed first-order decays. The clean first-order processes were applicable to the complete disappearance of the haloanisole cation radicals in acetonitrile, as established by the return of the absorbance to the base line in Figure 6B. It is important to reemphasize that the CT substitution of all the anisoles in this solvent led only to nitration (see Table I).

C. In *n*-hexane and benzene, the decay of the cation radicals derived from the CT excitation of the anisole complexes with TNM consistently followed first-order behavior (Table VIII). The first-order decays observed with every anisole in Table VIII must relate to the kinetics of aromatic alkylation, since this is the preponderant process in hydrocarbon solutions, irrespective of the substituent (see Table II).

VIII. Salt Effects on the Decay Kinetics for Aromatic Cation Radicals during CT Substitutions. In order to examine the effects of added salts on the kinetics of CT alkylation and nitration, we examined the decay of the transient cation-radical absorbance in the three solvents containing either the innocuous or common-ion salt TBAP or TBAT, respectively.

(35) See Hall and Gillespie in ref 32.

(36) Compare Masnovi in ref 15. Assuming a value of $\epsilon \sim 4000$ M^{-1} cm^{-1},[31] these rate constants correspond to $\sim 10^{10}$ M^{-1} s^{-1}.

Table VIII. Decay Kinetics of the Anisole Cation Radicals for CT Alkylation in Hydrocarbon Solution[a]

X-anisole		TNM,		time scale,		rate	λ,[d]
X	concn, M	M	solvent	μs	kinetics[b]	constant[c]	nm
4-methyl	0.10	0.42	C_6H_6	0.5–4	1°	1.6×10^6	460
	0.10	0.80	n-C_6H_{14}	0.05–0.4	1°	8.3×10^5	460
4-fluoro	0.2	1.2	n-C_6H_{14}	0–9	1°	8.6×10^5	490
4-chloro	0.20	1.2	n-C_6H_{14}	0–5	1°	1.6×10^6	490
4-bromo	0.20	1.2	n-C_6H_{14}	0–2	1°	2.9×10^6	510

[a] Following the 25-ps laser pulse at 532 nm at 25 °C. [b] First-order kinetics (1°). [c] First-order rate constant in s^{-1}. [d] Monitoring wavelength.

Table IX. Salt Effects on the Decay Kinetics for Aromatic Cation Radicals during CT Substitution[a]

solvent	ArH,[b] M	TNM, M	salt[c]	time scale, μs	kinetics[d]	rate constant[d]	λ, nm
CH_2Cl_2	0.10	0.42		10–100	2°	1.6×10^6	470
CH_2Cl_2	0.10	0.42	TBAP, (0.2 M)	10–200	2°	3.0×10^5	450
CH_2Cl_2	0.10	0.42	TBAT (0.01 M)	10–200	1°	3.0×10^4	470
MeCN	0.10	0.84		10–200	2°	2.5×10^5	450
MeCN	0.10	0.84	TBAP (0.2 M)	10–200	2°	3.3×10^5	450
MeCN	0.10	0.84	TBAT (0.01 M)	5–100	1°	2.7×10^4	470
C_6H_6	0.10	0.42		0.5–4	1°	1.6×10^6	460
C_6H_6	0.10	0.42	TBAP (0.01 M)[e]	2–30	2°	1.8×10^7	460
C_6H_6	0.10	0.42	TBAT (0.01 M)[e]	0.5–3	1°	9.8×10^5	460

[a] Following the 25-ps laser pulse at 532 nm at 25 °C. [b] 4-Methylanisole. [c] See Table III. [d] See Table VIII. [e] Saturated solution.

A. In dichloromethane, the disappearance of 4-methylanisole cation radical followed second-order kinetics in the presence of 0.2 M TBAP (Figure 7A). The second-order rate constant k_2 in Table IX differed by less than an order of magnitude from that obtained in salt-free dichloromethane (Figure 5B). Thus the salt effect on the decay kinetics was not nearly as dramatic as it was on the complete reversal in the products from CT alkylation to nitration (see entries 1–3, Table III). By way of contrast, the presence of the common-ion salt (0.2 M) TBAT altered the second-order kinetics to first-order kinetics (Figure 7B), despite the predominance of alkylation in both cases (see entries 1 and 4, Table III). It is important to note that this first-order rate process in dichloromethane containing TBAT was comparable to the first-order process observed in n-hexane and benzene without any salt (see entries 1 and 2, Table VIII).

B. In acetonitrile, the presence of the innocuous salt TBAP exerted little effect on the decay of the cation radical, the second-order rate constant being essentially unchanged (compare entries 4 and 5, Table IX). However, the presence of the common-ion salt altered the decay kinetics in acetonitrile from second-order to first-order behavior (entry 6), the magnitude of the first-order rate constant $k_1 = 2.7 \times 10^4\ s^{-1}$ being essentially the same as that obtained in dichloromethane with added TBAT (see entry 3, Table IX).

C. In benzene, the first-order kinetics observed in the absence of salt (Table VIII) was replaced by second-order kinetics when 0.01 M of the innocuous salt TBAP was present (see entry 8, Table IX). A slight negative salt effect was observed in the presence of the common-ion salt, but the decay pattern remained first order (see entry 9).

IX. Deuterium Kinetic Isotope Effects for Charge-Transfer Substitutions. The kinetic isotope effects for the charge-transfer substitutions of 4-methylanisole and 4-methylanisole-*2,6-d*$_2$ were also determined in two ways.

A. The kinetics of CT alkylation were measured spectrophotometrically in dichloromethane by following the disappearance of the CT band in the presence of excess tetranitromethane. The pseudo-first-order rate process measured at three wavelengths (490, 520, and 550 nm) under conditions of constant irradiation at λ > 425 nm afforded the rate constants $k_H = 1.28 \times 10^{-2}\ min^{-1}$ and $k_D = 1.23 \times 10^{-2}\ min^{-1}$ for 4-methylanisole and 4-methylanisole-*2,6-d*$_2$, respectively. The ratio $k_H/k_D = 1.04$ represented, within experimental error, a kinetic isotope effect of unity for CT alkylation.

B. The kinetic isotope effect for CT nitration was evaluated by the direct competition between equimolar amounts of 4-methylanisole and 4-methylanisole-*2,6-d*$_2$ in acetonitrile containing excess tetranitromethane. After CT irradiation at λ > 425 nm, the relative amounts of the disappearance of methylanisole and its deuteriated analogue were determined by GC–MS analysis using the molecular ions with m/z = 122 and 124, respectively. Similarly, the relative amounts of the nitration products from the protio- and deuterioanisoles were determined from the relative abundances of the molecular ions with m/z = 167 and 168, respectively, for the nitroanisoles and m/z = 153 and 154, respectively, for the nitrophenols. The ratios obtained at various conversions yielded an average kinetic isotope effect of unity for CT nitration (see Table XI, Experimental Section).

Discussion

The direct excitation of the charge-transfer bands of the electron donor–acceptor complexes of arenes provides a unique opportunity to examine the ambivalent character of the aromatic cation radical, as it suffers annihilation by collapse with either an anion $A:^-$ or a radical $R^\bullet$ in eq 1. Most noteworthy is the pronounced modulation of this competition by solvent polarity and by added salts. Thus the efficient collapse of ion pairs in nonpolar solvents is completely subverted to radical-pair collapse by a simple change to polar solvents, i.e.

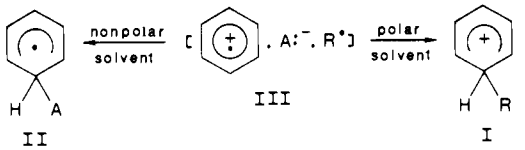

(12)

where $A:^-$ and $R^\bullet$ represent $C(NO_2)_3^-$ and $NO_2^\bullet$, respectively, in this study. Strikingly, the mere presence of low concentrations of innocuous salts such as the quaternary ammonium perchlorates (e.g., TBAP) in nonpolar solvents effects the same diversion from ion-pair collapse to radical-pair collapse, i.e.

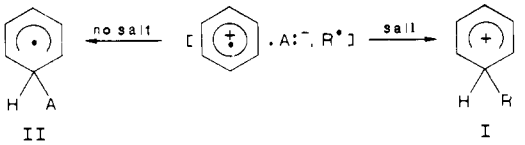

(13)

To delineate such a remarkable solvent and salt effect on the behavior of aromatic cation radicals ($ArH^{\bullet+}$), we proceed from the relevant photophysical and photochemical processes previously established by time-resolved spectroscopy of the CT excitation of aromatic (ArH) complexes with tetranitromethane (TNM).[8,37]

(37) See also: (a) Hilinski, E. F.; Masnovi, J. M.; Kochi, J. K.; Rentzepis, P. M. *J. Am. Chem. Soc.* **1984**, *106*, 871. (b) Masnovi, J. M.; Hilinski, E. F.; Rentzepis, P. M.; Kochi, J. K. *J. Phys. Chem.* **1985**, *89*, 5387.

The generalized mechanism of the individual steps leading to formation of the caged triad III by charge-transfer excitation is summarized in Scheme I.

Scheme I

$$\mathrm{ArH} + \mathrm{C(NO_2)_4} \overset{K}{\rightleftharpoons} [\mathrm{ArH,\ C(NO_2)_4}] \quad (14)$$

$$[\mathrm{ArH,\ C(NO_2)_4}] \xrightarrow{h\nu_{CT}} [\mathrm{ArH^{\bullet +},\ C(NO_2)_4^{\bullet -}}] \quad (15)$$

$$[\mathrm{ArH^{\bullet +},\ C(NO_2)_4^{\bullet -}}] \xrightarrow{\text{fast}} \underset{\mathrm{III}}{[\mathrm{ArH^{\bullet +},\ NO_2^{\bullet},\ C(NO_2)_3^{-}}]} \quad (16)$$

In order to determine whether the general formulation outlined in Scheme I applies specifically to the substituted anisoles examined in this study, our first task is to establish the viability of the ion/radical triad III.

I. Spontaneous Evolution of Ion/Radical Triad III by CT Excitation. The rapid formation of the EDA complex is illustrated in Figure 2, and it occurs within the time of mixing the various anisoles with tetranitromethane. The limited magnitudes of the formation constant K in Table V indicates that the 1:1 complex [ArH, TNM] is formed in low steady-state concentrations.

Activation of the EDA complex by selective irradiation of the charge-transfer absorption bands (Figure 2B) results in photoinduced electron transfer according to eq 15, as predicted by Mulliken theory.[26,27] Irreversible fragmentation of $\mathrm{C(NO_2)_4^{\bullet -}}$ in eq 16 leads directly to ion/radical triad III (Figure 3). Comparison of the spectral transients from the CT irradiation of the EDA complex in dichloromethane (Figure 3) and in acetonitrile (Figure 4) indicates that the same species are formed. In other words, solvent polarity plays little or no role in the critical formation of ion/radical triad III. Moreover, the measured quantum yields Φ in Table IV show little variation with solvent polarity. The value $\Phi = 0.2$ for 4-methylanisole compares with $\Phi = 0.5$ and 0.7 for dialkoxybenzenes and anthracenes, respectively,[9,38] measured under the same experimental conditions. These high quantum yields relate directly to the efficiency of triad production in eq 16 relative to energy wastage by back electron transfer in eq 15. Indeed the trend $\Phi = 0.2$, 0.5, and 0.7 accords with the expected relative rates of back electron transfer based on the oxidation potentials $E^\circ = 1.67$, 1.30, and 1.23 V for 4-methylanisole, 1,4-dimethoxybenzene, and anthracene, respectively.[9,39]

The short lifetimes of less than 3 ps for $\mathrm{C(NO_2)_4^{\bullet -}}$ (as established in the anthracene studies[8]) indicate that triad species III are initially trapped within the solvent cage since this time scale precludes any competition from diffusional separation. Thus the vertical excitation of the EDA complex according to Scheme I ensures that $\mathrm{ArH^{\bullet +}}$ and $\mathrm{C(NO_2)_3^-}$ are born as a discrete, intimate ion pair in which the mean separation is largely dictated by the geometry extant in the precursor EDA complex.[40] Likewise, $\mathrm{ArH^{\bullet +}}$ and $\mathrm{NO_2^{\bullet}}$ exist in III as the geminate radical pair akin to those formed in bond homolysis.[41] Let us now focus on the pathways by which the caged triad suffers ion-pair and radical-pair collapse and ultimately leads to aromatic alkylation and nitration, respectively.

II. Transformation of Caged Triad III to Products of Aromatic Substitution. The excellent material balances obtained in Tables I and II demonstrate that caged triad III proceeds quantitatively to the aromatic products by one of two stoichiometries, viz.

$$\underset{\mathrm{III}}{[\mathrm{ArH^{\bullet +},\ C(NO_2)_3^{-},\ NO_2^{\bullet}}]} \rightarrow \mathrm{ArC(NO_2)_3} + \mathrm{HNO_2} \quad (17)$$

$$\hookrightarrow \mathrm{ArNO_2} + \mathrm{HC(NO_2)_3} \quad (18)$$

Under conditions in which alkylation and nitration are observed simultaneously, combination of eq 17 and 18 accounts for the complete material balance for CT substitution.

Since aromatic alkylation clearly derives from the coupling of the aromatic cation with the trinitromethide anion, the pathway for eq 17 is designated as *ion-pair collapse*. Analogously, the pathway to aromatic nitration in eq 18 is identified as *radical-pair collapse*.

The absence of a deuterium kinetic isotope effect in either aromatic alkylation or nitration (vide supra) effectively precludes the loss of the aromatic hydrogen as $\mathrm{H^{\bullet}}$ or $\mathrm{H^+}$ in a rate-limiting step. Accordingly, we formulate a two-step process in which the rate of aromatic alkylation is determined by the rate constant k_{ip} from prior *ionic* addition, i.e.

Scheme II

$$\underset{\mathrm{III}}{[\mathrm{ArH^{\bullet +},\ C(NO_2)_3^{-},\ NO_2^{\bullet}}]} \xrightarrow{k_{ip}} \underset{\mathrm{II}}{\mathrm{^{\bullet}ArH(C(NO_2)_3)}} + \mathrm{NO_2^{\bullet}} \quad (19)$$

$$\mathrm{II} + \mathrm{NO_2^{\bullet}} \xrightarrow{\text{fast}} \mathrm{ArC(NO_2)_3} + \mathrm{HNO_2} \quad (20)$$

The σ-adduct II formed in eq 19 is analogous to the intermediates in homolytic alkylation.[7,42] As such, the hydrogen-atom transfer in eq 20 is expected to be facile, and this conclusion accords with the absence of a deuterium isotope effect in CT alkylation.[43]

By an analogous formulation, the rate of aromatic nitration is determined by the rate constant k_{rp} from *homolytic* addition, i.e.

Scheme III

$$\underset{\mathrm{III}}{[\mathrm{ArH^{\bullet +},\ C(NO_2)_3^{-},\ NO_2^{\bullet}}]} \xrightarrow{k_{rp}} \underset{\mathrm{I}}{\mathrm{^{+}ArH(NO_2)}} + \mathrm{C(NO_2)_3^-} \quad (21)$$

$$\mathrm{I} + \mathrm{C(NO_2)_3^-} \xrightarrow{\text{fast}} \mathrm{ArNO_2} + \mathrm{HC(NO_2)_3}$$

The σ-adduct I formed in eq 21 is the Wheland intermediate in electrophilic nitration.[6] As such, it relates directly to the classical studies of Melander,[44] who first established the rapid, irreversible loss of proton from the Wheland intermediate.[45]

The dichotomy between aromatic alkylation and nitration as described in Schemes II and III provides the basis for understanding the extraordinary solvent and salt effects on the behavior of transient aromatic cation radicals. In order to carry out the mechanistic analysis, we briefly refer to our earlier studies in which the dynamics of ion pairs similar to that in III were dissected quantitatively.[15] Of particular concern is the segregation of the ion and radical fragments in III, especially with regard to diffusive separation. This is accomplished by first considering the dynamics of ion-pair separation. Such a priority is dictated by the dominance of the inherent Coulombic interactions in enthalpic considerations and the large driving force provided by the neutralization of the opposite charges in the formation of adduct II in eq 19.

The earlier time-resolved spectroscopic studies[15] established the existence of three successive rate profiles of ion pairs. These were ascribed to (a) the fast first-order decay (k_1) of the first-formed, intimate ion pair $[\mathrm{ArH^{\bullet +},\ C(NO_2)_3^-}]$ to the "loose" or solvent-separated ion pair $[\mathrm{ArH^+||C(NO_2)_3^-}]$, which subsequently suffer (b) another first-order, but slower decay (k_1') to the free ions $\mathrm{ArH^{\bullet +}}$ and $\mathrm{C(NO_2)_3^-}$, and finally (c) the second-order diffusive combination (k_2) of the separated ions. The ion-pair dynamics summarized in Scheme IV drew upon the pioneering studies of

(38) Masnovi, J. M.; Kochi, J. K. *J. Org. Chem.* **1985**, *50*, 5245.
(39) Masnovi, J. M.; Seddon, E. A.; Kochi, J. K. *Can. J. Chem.* **1984**, *62*, 2552.
(40) For the mean separation in the EDA complexes of the type described here, see: (a) Fukuzumi, S.; Kochi, J. K. *J. Phys. Chem.* **1980**, *84*, 608 and related papers. (b) See also ref 37b and: Blackstock, S. C.; Kochi, J. K. *J. Am. Chem. Soc.* **1987**, *109*, 2484.
(41) Koenig, T.; Fischer, H. In *Free Radicals*; Kochi, J. K., Ed.; Wiley: New York, 1973; Vol. 1, p 157ff.
(42) Nonhebel, D. C.; Walton, J. C. *Free Radical Chemistry*; Cambridge University Press: London, 1974; p 447ff.
(43) For experimental indications of an addition–elimination sequence for hydrogen loss, see the Experimental Section.
(44) (a) Melander, L. *Arkiv. Kemi* **1950**, *2*, 211. (b) Melander, L. *Ark. Kemi* **1957**, *11*, 77. See also: Melander, L. *Isotope Effects on Reaction Rates*; Ronald Press: New York, 1960.
(45) For a recent summary of aromatic nitration by an electron-transfer mechanism involving radical-pair collapse, see: Eberson, L. *Acc. Chem. Res.* **1987**, *20*, 53.

Scheme IV

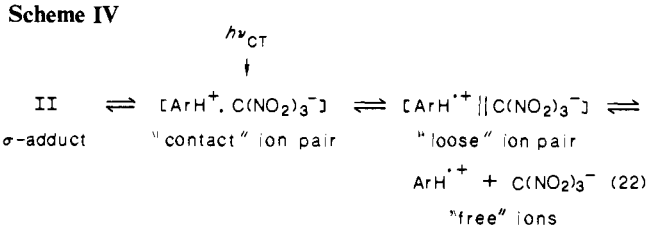

Winstein and co-workers for solvolytic processes.[46-49] As such, the quantitative treatments of the "special salt" and common-ion effects, as represented by TBAP and TBAT, respectively, provide important support for the substantiation of this formulation. Accordingly, let us consider how the time-resolved spectroscopic studies delineate the role of both the solvent polarity and added salts in CT alkylation as well as in CT nitration. Before doing so, however, it is important to emphasize that the clean stoichiometries in Tables I and II for eq 19 and 21, respectively, allow us to examine the rates of these processes by spectrally following the disappearance of only the aromatic cation radical. Thus the stoichiometry for alkylation (eq 3) and nitration (eq 4) demands the concomitant disappearance of an equivalent amount of the anion $C(NO_2)_3^-$ and the radical $NO_2^\bullet$, respectively.

III. Solvent and Salt Effects in the Mechanism for CT Alkylation by Ion-Pair Annihilation. Ion-pair annihilation in eq 19 is favored by nonpolar solvents, as indicated by the high yields of the alkylation products in Table II. The decay pattern of the spectral transient provides interesting insight as to how the ion-pair collapse occurs, since there are large changes with even minor variations in the solvent and with small amounts of added salt (Table III).

In hydrocarbon solvents (*n*-hexane and benzene), the rate profile for eq 19 (Scheme II) follows first-order kinetics (Table VIII), which reflect the ion-pair collapse from the geminate ions originally present in III.[50] However, in slightly more polar solvents such as dichloromethane,[51] the rate profile for eq 19 follows a different kinetics behavior (see Table VI). Indeed the magnitudes of the second-order rate constants in dichloromethane are reminiscent of those obtained earlier for the combination of the separate, free ions.[15] Such a diverse behavior parallels the increased lifetimes of ions in the more polar medium such as dichloromethane relative to hexane. Under these circumstances, the enhanced diffusive separation of the ion pair in III will be reflected in the change in the kinetics from first-order to second-order behavior.[53] In terms of Scheme IV, the change in kinetics from hydrocarbon solvents (Table VIII) to dichloromethane (Table VI) represents a change in mechanism for alkylation from the collapse of the intimate or solvent-separated ion pair $[ArH^{\bullet+}\|C(NO_2)_3^-]$ to diffusive combination of $ArH^{\bullet+}$ and $C(NO_2)_3^-$.[54] In accord with

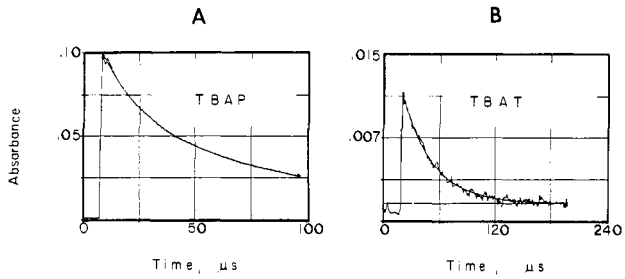

Figure 7. Salt effects on the decay of the 4-methylanisole cation radical from the CT irradiation of 0.1 M 4-methylanisole and 0.4 M TNM in dichloromethane containing (A) 0.2 M TBAP and (B) 0.01 M TBAT.

this conclusion, it is noteworthy that the series of first-order rate constants k_1 in Table VIII follow essentially the same trend as the second-order rate constants k_2 in Table VI.[55] Both rate constants (i.e., log k_1 and log k_2) reflect the energetics of ion-pair collapse in eq 19. The relatively large gap between the reactivity of the *p*-methylanisole and *p*-fluoroanisole cations parallels the difference in the oxidation potential of the parent anisoles; i.e., E° = 1.67 and 2.12 V, respectively.[56] As such, it largely represents the difference in the stabilities of the anisole cation radicals.[57] By comparison the highly stabilized cation radical from the CT excitation of *p*-methoxyanisole with E° = 1.30 V is incapable of ion-pair collapse with trinitromethide anion.[9] We thus conclude from the decay kinetics and from the products that the primary distinction between benzene (or hexane) and dichloromethane as solvents for ion-pair annihilation arises from differences in dielectric constants that allow increased separation of the ions in the more polar solvent.[51]

The effects of added salt on the decay kinetics of the ion pair in III can be interpreted in terms of the "special salt" and "common-ion" effects on the ion-pair equilibria in Scheme IV. For example, the presence of the innocuous salt TBAP in benzene alters the decay from first-order to second-order kinetics. (See entries 8 and 9, Table IX.) In terms of Scheme IV, the effect of added TBAP is to exchange the active ion pair with an inactive ion pair, i.e.

$$\underset{\text{active ion pair}}{[ArH^{\bullet+}, C(NO_2)_3^-]} + [Bu_4N^+, ClO_4^-] \rightleftharpoons \underset{\text{inactive ion pair}}{[ArH^+, ClO_4^-]} + [Bu_4N^+, C(NO_2)_3^-] \quad (23)$$

which is tantamount to ion-pair separation by the "special salt" effect.[15] This change is also reflected in decreased amounts of CT alkylation (see Table III, entry 10). The fact that CT alkylation is not completely wiped out by TBAP indicates that the ion-pair exchange in eq 23 is not thorough in the highly nonpolar hydrocarbon media. Conversely, ion-pair separation is completely inhibited by the presence of TBAT—the decay process maintaining first-order kinetics as a result of common-ion suppression, i.e.

$$\underset{\text{free}}{ArH^+} + [Bu_4N^+, C(NO_2)_3^-] \rightleftharpoons \underset{\text{active ion pair}}{[ArH^{\bullet+}, C(NO_2)_3^-]} + Bu_4N^+ \quad (24)$$

As expected, this is reflected in exclusive CT alkylation (entry 11, Table III).

The effects of added salts on the decay profile in dichloromethane are qualitatively the same as those described above in hexane. Thus the second-order kinetics observed in this more polar solvent (Table IV) persists in the presence of added TBAP. However, the product analysis in Table III (entry 2) shows the complete absence of CT alkyiation! The second-order kinetics

(46) (a) Winstein, S.; Klinedinst, P. E., Jr.; Robinson, G. C. *J. Am. Chem. Soc.* **1961**, *83*, 885. (b) Winstein, S.; Klinedinst, P. E., Jr.; Clippinger, E. *J. Am. Chem. Soc.* **1961**, *83*, 4986. (c) Winstein, S.; Robinson, G. C. *J. Am. Chem. Soc.* **1958**, *80*, 169 and related papers. For reviews, see: (d) Harris, J. M. *Prog. Phys. Org. Chem.* **1974**, *11*, 89. (e) Szwarc, M., Ed. *Ions and Ion Pairs in Organic Reactions*; Wiley-Interscience: New York, 1974; Vol. 2, Chapter 3, p 247ff.

(47) Weiner, H.; Sneen, R. A. *J. Am. Chem. Soc.* **1965**, *87*, 287, 292. Sneen, R. A.; Larsen, J. W. *J. Am. Chem. Soc.* **1966**, *88*, 2593. Ogg, R. A., Jr.; Polanyi, M. *Trans. Faraday Soc.* **1935**, *31*, 604.

(48) (a) Goering, H. L.; Briody, E. G.; Levy, J. F. *J. Am. Chem. Soc.* **1963**, *85*, 3059. Goering, H. L.; Levy, J. F. *J. Am. Chem. Soc.* **1964**, *86*, 120. Young, W. G.; Winstein, S.; Goering, H. L. *J. Am. Chem. Soc.* **1951**, *73*, 1958. (b) Crampton, M. R.; Grunwald, E. *J. Am. Chem. Soc.* **1971**, *93*, 2987.

(49) See: Shiner, V. J., Jr. In *Isotope Effects in Chemical Reactions*; Collins, C. J., Bowman, N. W., Eds.; Von Nostrand Reinhold: New York, 1970.

(50) In this discussion we have not distinguished between intimate and solvent-separated ion pairs.[15]

(51) Based on the dielectric constant of *n*-hexane (1.89), benzene (2.28), dichloromethane (9.08), and acetonitrile (37.5).[52]

(52) Dean, J. A., Ed. *Lange's Handbook of Chemistry*, 12th ed.; McGraw-Hill: New York, 1979, p 10-103f.

(53) For a related phenomenon, see ref 15.

(54) By microscopic reversibility, the latter proceeds to the σ-adduct II via the solvent-separated and contact ion pairs. See also footnote 34 in ref 15.

(55) The different amounts of byproducts must be taken into account for a direct comparison.

(56) Kuchynka, D. J., unpublished results.

(57) It is likely that all the neutral anisoles have more or less the same heats of formation.

Table X. Kinetics of Electron-Transfer Nitration

$E°$,[a] V vs. SCE	X-anisole X	kinetics[b]	rate constant[c]
1.30	4-methoxy	2°	1.0×10^4
1.67	4-methyl	2°	2.5×10^5
2.12	4-fluoro	1°	1.9×10^4
2.00	4-chloro	1°	2.4×10^4
1.78	4-bromo	1°	3.7×10^4

[a] In acetonitrile containing 0.1 M TBAP at 25 °C. [b] 2° and 1° represent second- and first-order decays, respectively. [c] In units of A^{-1} s^{-1} for second-order kinetics and s^{-1} for first-order kinetics.

must therefore be associated with CT nitration, even at low levels (0.01 M) of TBAP (entry 3). Furthermore, the presence of the common-ion salt TBAT is inadequate to completely counter this large positive salt effect (see entry 4, Table III).

The increased efficiency with which added salts affect the ionic ion-pair equilibria (Scheme IV) in dichloromethane relative to hexane can be attributed to the slightly greater polar properties of the solvent (vide supra). This change presumably acts on the ion-pair exchange such as that in eq 23, which effectively separates the cationic $ArH^{\bullet +}$ from the anionic trinitromethide. The aggregation of ion pairs, particularly in the highly nonpolar (and poorly solvating) hydrocarbons,[58] accounts for the decreased efficiency of such ion-pair exchange.

IV. Mechanism of CT Nitration by Radical-Pair Annihilation. In the absence of competition for ion-pair collapse as described in the preceding section, the CT excitation of the EDA complex leads only to aromatic nitration. This is particularly evident with electron-rich arenes such as *p*-methoxyanisole which afford highly persistent cation radicals incapable of ion-pair annihilation with trinitromethide anion in all solvents, including hexane.[9] As a result, quantitative yields of nitration products are always obtained with a variety of dialkoxybenzenes upon the CT irradiation of their EDA complexes with tetranitromethane.

With the more reactive aromatic cation radicals examined in this study, the competition from ion-pair separation becomes increasingly more important only in highly polar solvents such as acetonitrile.[33] Indeed the dramatic change in the course of CT substitution from aromatic alkylation to nitration parallels the change in solvent from dichloromethane to acetonitrile (compare Tables I and II).

According to Scheme III, the mechanism of CT nitration depends on the particular pathway by which $ArH^{\bullet +}$ encounters $NO_2^{\bullet}$. Indeed, the decay pattern of the spectral transients for nitration in acetonitrile (Table VII) is strikingly dependent on the stability of the aromatic cation radicals as measured by the one-electron oxidation potentials $E°$ of the arene, i.e.

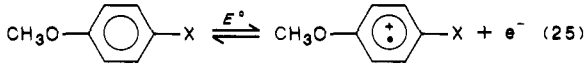

(25)

The direct comparison of $E°$ in Table X focuses on the substantial effect of substituents (X) on the inherent stability of the aromatic cation radicals.[57]

The decay of the spectral transients for nitration in eq 21 (Scheme III) is a reflection of the stability of the aromatic cation radical. For example, the cation radical from *p*-methylanisole decays by second-order kinetics in acetonitrile, similar to the kinetic behavior of the long-lived cation radical from *p*-methoxyanisole.[9] The large difference in the rates of diffusive combination with $NO_2^{\bullet}$ in Table X (see column 4) corresponds to their relative stabilities as measured by $\Delta E° = 8.5$ kcal mol^{-1} of the parent arenes (column 1).

There is a further, larger gap of $\Delta E° = 10.4$ kcal mol^{-1} which separates the stabilities of the cation radicals of *p*-methylanisole and *p*-fluoroanisole, the least reactive haloanisole. Strikingly, every member of the family of *p*-haloanisole cation radicals reacts with $NO_2^{\bullet}$ by first-order kinetics. This decay pattern strongly suggests that the CT nitration occurs by the cage collapse of the geminate radical pair $[ArH^{\bullet +}, NO_2^{\bullet}]$ prior to diffusive separation, except when the anisole cation is a relatively stabilized species such as those with *p*-methyl and *p*-methoxy substituents. Such a mechanism for nitration implies that polar solvents act selectively to preferentially separate the anion from the cation and $NO_2^{\bullet}$ in the geminate triad III. This conclusion is also consistent with the marked effect of added innocuous salt TBAP in the less polar solvent dichloromethane. It is noteworthy that the second-order rate constant for nitration under these conditions (Table IX, entry 2) is the same as that obtained in acetonitrile (entry 4).[60]

V. Comments on the Regiospecificity in the CT Alkylation and Nitration. The isomer distributions in CT alkylation and nitration are established in Schemes II and III during ion-pair and radical-pair collapse according to eq 19 and 21, respectively. Since the driving forces for both of these processes are likely to be exergonic, the transition states for the formation of the aromatic σ-adducts I and II will bear a strong resemblance to the aromatic cation radical.[59] As such, the charge and electron density in $ArH^{\bullet +}$ will be an important factor in determining the positional selectivity in the aromatic ring.[61] As a first approximation, the regiospecificity in ion-pair and radical-pair collapse should be the same, siince the site of highest positive charge in $ArH^{\bullet +}$ will also be the site of highest electron spin density. The latter are determined from EPR spectra, which show that these locations in the cation radicals of anisole and its derivatives are concentrated at the ortho and para positions relative to the methoxy group,[3] e.g.

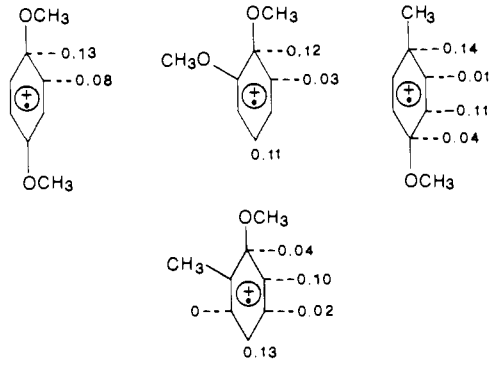

Examination of the products in Tables I and II indeed shows that CT nitration and alkylation both occur at sites ortho and para to the methoxy group. However, the absence of the ortho isomers during CT alkylation of anisole as well as 2- and 3-methylanisoles in Table II indicates that the introduction of the bulky trinitromethyl group is somewhat subject to steric hindrance. Otherwise, the collapse of the ion pair $[ArH^{\bullet +}, C(NO_2)_3^-]$ and the radical pair $[ArH^{\bullet +}, NO_2^{\bullet}]$ to the σ-adducts II and I, respectively, leads

(58) Compare: Goodson, B. E.; Schuster, G. B. *J. Am. Chem. Soc.* **1984**, *106*, 7254.

(59) (a) Hammond, G. S. *J. Am. Chem. Soc.* **1955**, *77*, 334. (b) See also: Lowry, T. H.; Richardson, K. S. *Mechanism and Theory in Organic Chemistry*, 2nd ed.; Harper and Row: New York, 1981, p 197ff.

(60) (a) The curious first-order kinetics in acetonitrile with added TBAT (Table IX, entry 6) was also observed in the nitration of 1,4-dimethoxybenzene.[9] Such a kinetic behavior could arise from an association of $NO_2^{\bullet}$ with $C(NO_2)_3^-$ in geminate species. (b) We find the first-order rate constants in Table X to be unexpectedly slow, which suggests the presence of a barrier to the radical combination. The interesting question then arises as to why the ion-radical pair $[ArH^{\bullet +}, NO_2^{\bullet}]$ persists for so long ($\tau \sim 25$ μs). A referee has suggested the possibility that they may receive a degree of stabilization by a CT interaction, which is the microscopic reverse of the CT interaction between the free arene and NO_2^+. We hope that further studies with other aromatic donors will delineate the structural dependence of this first-order rate constant and help to point out the mechanistic relevance to electrophilic aromatic substitution. In the latter connection, the alternative (circuitous) possibility of back electron transfer of the ion-radical pair to regenerate $[ArH, NO_2^+]$ followed by addition to form the Wheland intermediate is not supported in the gas-phase system (see: Schmitt, R. J.; Buttrill, S. E., Jr.; Ross, D. S. *J. Am. Chem. Soc.* **1984**, *106*, 926). The detailed comparison of the isomer distributions of the products derived from CT nitration and electrophilic nitration (HNO_3) of various aromatic compounds will be presented separately.

(61) For a discussion of this point, see: Fukuzumi, S.; Kochi, J. K. *J. Am. Chem. Soc.* **1981**, *103*, 7240.

to the same positional selectivity in CT alkylation and nitration.[62]

The σ-adduct I arising from the radical-pair collapse is the Wheland intermediate in electrophilic nitration. Thus it is worth noting that the byproducts from CT nitration in Table I are strongly reminiscent of the byproducts reported in electrophilic nitration of the anisoles with nitric acid. In particular, the demethylation of the methoxy group to afford nitrophenols and the transbromination of 4-bromoanisole to afford a mixture 4-nitroanisole and 2,4-dibromoanisole are both symptomatic of radical-pair collapse at the ipso positions. These produce the σ-adducts I, which are akin to the Wheland intermediates known to undergo such transformations,[17-20] i.e.

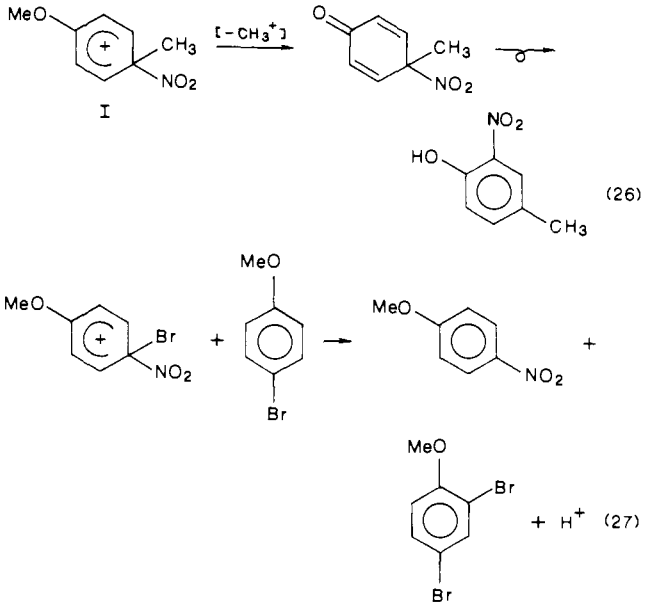

We hope that further studies will establish the direct relationship between the σ-adducts I derived from the radical-pair collapse of [$ArH^{\bullet +}$, $NO_2^{\bullet}$] and the Wheland intermediate formed in electrophilic nitration.[60]

Summary and Conclusions

The charge-transfer irradiation of aromatic complexes yields an intimate ensemble of a cation, anion, and radical as the solvent-caged triad [$ArH^{\bullet +}$, $C(NO_2)_3^-$, $NO_2^{\bullet}$] (III). The temporal evolution of geminate triad III is strongly dependent on the polarity of the medium. Thus the predominant process in nonpolar solvents (benzene, *n*-hexane, dichloromethane) is the efficient ion-pair collapse of III, leading to aromatic (trinitro)alkylation [i.e., $ArC(NO_2)_3$ and HNO_2 in eq 3]. By contrast, polar solvents (acetonitrile) promote radical-pair collapse of III, leading exclusively to aromatic nitration [i.e., $ArNO_2$ and $HC(NO_2)_3$ in eq 4]. The presence of the added innocuous salt TBAP is sufficient to discourage ion-pair collapse, and aromatic nitration is the exclusive fate of III in dichloromethane.

Such diverse fates of caged triad III can be accommodated within a single mechanistic framework by considering the primacy of the ion-pair equilibria in Scheme IV, especially as it is modulated by solvent polarity and added salts. This analysis derives from the decay kinetics of the transients produced upon the 25-ps laser-pulse excitation of the EDA complexes. Thus the first-order decay in hexane (Table VIII) relates to the direct collapse of the ion pair [ArH^+, $C(NO_2)_3^-$] to the σ-adduct II, whereas the second-order decay in dichloromethane represents the (re)combination of the free $ArH^{\bullet +}$ and $C(NO_2)_3^-$ after diffusive separation in the more polar medium. The effects of added salt can be similarly analyzed in terms of ion-pair exchange in Scheme IV, as modulated by "special salt" (eq 23) and "common-ion" (eq 24) effects.

The comparison of the behavior of various para-substituted anisoles shows that ion-pair collapse is strongly dependent on the stability of the cation radical, being nonexistent with the highly stabilized *p*-methoxyanisole cation radical.[9] The rates of ion-pair collapse of 4-substituted anisole cations increase in the order methyl < fluoro < chloro < bromo (Tables VI and VIII), in line with the oxidation potentials E° of the parent anisole. Moreover, the rates of radical-pair collapse to the σ-adduct I also increase in the same order, but with a change in the decay behavior from second-order kinetics for *p*-methylanisole to first-order kinetics for all the haloanisoles. The latter points to the importance of a geminate process for radical-pair collapse from III with reactive cation radicals. Clearly, further studies are required to substantiate this interesting facet of solvent effects on the diffusive behavior of cations, anions, and neutral radicals. Nonetheless the complex solvent effect on the decay patterns of ion/radical triad III in Tables VI–VIII can be accounted for in a consistent manner if ion-pair collapse in eq 19 is the preferred process, except for aromatic cation radicals, which are stabilized by electron-donor substituents (e.g., *p*-methyl and *p*-methoxy), by solvation (e.g., acetonitrile), or by added salt (TBAP).

Experimental Section

Materials. 4-Fluoroanisole, 2-methylanisole, 5-methyl-2-nitroanisole, 3-methyl-2-nitroanisole, and 3-methyl-4-nitroanisole from Aldrich, *p*-chloroanisole, *p*-bromoanisole, and *m*-nitroanisole from Eastman, and *o*- and *p*-nitroanisole from Matheson Coleman and Bell were used as received. Anisole and 4-methylanisole (Aldrich) were purified by distillation prior to use. Tetranitromethane was prepared by the nitration of acetic anhydride (MCB).[63] Hexane (EM Science), benzene (Fisher), dichloromethane (Fisher), and acetonitrile (Burdick and Jackson) were spectral grade solvents. 4-Methylanisole-*2,6-d*$_2$ was prepared by refluxing it in a 1:1 (by volume) mixture of trifluoroacetic anhydride and D_2O overnight.[64] The procedure was repeated three times to effect >99% isotopic incorporation by mass spectral analysis. A pure sample of 2,6-dideuterio-4-methylanisole was obtained by distillation. Reinecke's salt used for actinometry was from Aldrich. The commercially available ammonium salt was converted to the potassium salt by dissolving it in warm water, adding excess solid potassium nitrate, cooling, and filtering. The potassium salt was recrystallized from warm water and dried over P_2O_5 in a vacuum desiccator. All of these operations were carried out in dim red light. The various products of CT nitration of the anisoles were prepared independently by treatment of the anisoles with fuming nitric acid in acetic anhydride at 0 °C.[65] An authentic sample of 2,4-dibromoanisole was prepared as follows. Bromine (2 mmol, 0.1 mL) was added to a well-stirred solution of 4-bromoanisole (2 mmol, 0.25 mL) in acetic acid (2 mL), and the mixture was left overnight. The crude reaction mixture was diluted with ether, and the ethereal solution was washed with 10% aqueous sodium hydroxide until the washings were alkaline. The ether layer was dried over $MgSO_4$. Evaporation of ether yielded 2,4-dibromoanisole as a white crystalline solid. Recrystallization of the crude product from a mixture of ether–hexane yielded pure 2,4-dibromoanisole. 2,4-Dibromoanisole: mp 62 °C (lit:[66] mp 61.5 °C); ^1H NMR ($CDCl_3$) δ 7.66 (d, 1 H, H-3, J = 2.4 Hz), 7.37 (dd, 1 H, H-5, J = 2.4 Hz, 8.5 Hz), 6.76 (d, 1 H, H-6, J = 8.5 Hz), 3.87 (s, 3 H, OCH_3); MS (70 eV) m/z 268 (47), 266 (100), 264 (49), 253 (24), 251 (49), 249 (26), 225 (17), 223 (35), 221 (18), 172 (11), 170 (11), 75 (19), 74 (18), 63 (51), 62 (25), 61 (13). Tetrabutylammonium trinitromethide was prepared from nitroform and tetrabutylammonium hydroxide (Aldrich) as reported earlier.[15] The commercially available tetrabutylammonium perchlorate (Pfaltz & Bauer) was purified by recrystallization from ethyl acetate.

Instrumentation. The UV–vis spectra were recorded on a Hewlett-Packard 8450A diode-array spectrometer. A Nicolet 10DX FTIR spectrometer was used to record all IR spectra. NMR spectra were recorded on a JEOL FX90Q spectrometer operating at 90 MHz for ^1H and 22.5 MHz for ^{13}C. Proton chemical shifts are reported in ppm downfield from a TMS internal standard. Carbon-13 chemical shifts are reported in ppm, and either the resonance for TMS (δ_C = 0) or the center of the multiplet resonance for the solvent (e.g., $CDCl_3$ = 77.0 ppm) was taken as reference. The NMR data are reported in the following format: chemical shift in ppm (multiplicity, number of protons, assignment of

(62) Based on the assumption that eq 19 and 21 are irreversible.

(63) Liang, P. *Organic Syntheses*; Wiley: New York, 1955; Collect. Vol. III, p 803. See also: Bielski, B. H. J.; Allen, A. O. *J. Phys. Chem.* **1967**, *71*, 4544.

(64) Lau, W.; Kochi, J. K. *J. Am. Chem. Soc.* **1986**, *108*, 6720.

(65) Sankararaman, S., to be published. Compare the thermal nitrations of dialkoxybenzenes in ref 9.

(66) Hashimoto, T. J. *Pharm. Soc. Jpn.* **1960**, *80*, 1344.

proton, coupling constant in hertz). The gas chromatographic (GC) analyses were performed on a Hewlett-Packard 5790A chromatograph using a 12.5 M SE 30 (cross-linked methylsilicone) capillary column. The liquid chromatographic analyses were performed either on an IBM LC 9533 ternary system using a C-18 reverse-phase columnn or on a Waters 6000 A system using a silica gel column. The GC–MS analyses were carried out on a Hewlett-Packard 5890 chromatograph interfaced to a HP5970 mass spectrometer (EI, 70 eV). Melting points were determined on a Mel-Temp (Laboratory Devices) apparatus and are uncorrected.

Time-resolved differential absorption spectra in the microsecond time scale were obtained on a laser flash system. It utilized the 532-nm second harmonic 10-ns pulses from a Quantel YG 481 Nd:YAG laser, which was monitored with a 150-W xenon lamp. A Spex minimate monochromator, Hamamatsu R928 NM photomultiplier tube, and either a Tektronix R7912 digitizer or a Biomation 8100 waveform recorder were used for probe assembly.[67] Signals were digitized, averaged, and interfaced with a Digital Equipment PDP 11/70 computer for analysis.[68] For the differential absorption spectra and decay kinetics in the nanosecond time scale the 532-nm second harmonic from a mode-locked Nd:YAG (Quantel) laser with a 200-ps pulse was used.

For the disappearance of the arene cation radicals, in each experiment 10–30 shots were averaged to obtain the decay curves. The reaction order of the decay was established by a linear least-squares computer fit of the observed decrease of the absorbance (A) with time as a function of either ln A or A^{-1} for the first or second order, respectively. The intensity of the laser pulse was altered by using wire mesh filters to confirm the reaction order of the decay. Under these conditions for a true first-order decay, the rate constant and the half-life remained unchanged with change in the intensity of the laser pulse. For a true second-order decay the half-life doubled and the rate constant remained unchanged when the intensity of the laser pulse was halved. For more complicated decays, a fitting routine was utilized to extract the rate constants sequentially by determining the rate of the slower component initially.[15]

Steady-state photochemical irradiations were performed by using a focused beam from either a 500-W Osram (HBO-2L2) high-pressure Hg lamp or a 1000-W Hanovia (977B0010) Hg–Xe lamp. The light passed through an IR water filter coupled to a Corning CS-3-72 (425 nm) or CS-3-70 (500 nm) glass cutoff filter. Irradiations were performed either in a 1-cm quartz cell or a Pyrex Schlenk tube immersed in cold water contained in a Pyrex dewar.

Formation of Radical Cations of 4-Haloanisoles by Pulse Radiolysis. The radical cations of 4-haloanisoles were produced by pulse radiolysis, following the procedure reported by Steenken and co-workers.[31] A Van de Graaff type electron generator delivering 800-ns single pulses of ≅4-MeV electrons with a dose rate of 50 rad ns^{-1} A^{-1} was used as the electron source. A 150-W xenon lamp was used as the monitor. A Spex minimate monochromator, a Hamamatsu R928 NM photomultiplier tube, and a Tektronix R7912 digitizer were used for the probe assembly. The probe assembly was interfaced with a Digital Equipment PDP 11/70 computer for analysis.

In pulse radiolysis experiments the water used was distilled from potassium permanganate. A stock solution containing 10^{-3} M thallous nitrate at pH 2.4 was prepared. The pH of the solution was adjusted with perchloric acid. Aqueous solutions containing 10^{-4} M 4-haloanisoles were prepared by dissolving the 4-haloanisoles in the stock solution. The solutions were saturated with N_2O. In a typical experiment 30 mL of an aqueous solution containing 10^{-3} M thallous nitrate and 10^{-4} M 4-haloanisole, saturated with N_2O at pH 2.4, was taken in a hypodermic syringe. The syringe was attached to a flow cell. Fresh solution was injected into the cell after each pulse of electrons. The differential absorption spectra of the radical cation of the 4-haloanisoles were obtained by scanning from 300 to 800 nm at 10-nm intervals. The radical cation spectrum of 4-chloro- and 4-bromoanisole obtained by this method had λ_{max} at 460 and 520 nm, respectively.

Determination of the Formation Constants of the EDA Complexes from Anisoles and TNM. In a typical experiment, a solution containing 0.1 M anisole in dichloromethane or acetonitrile (1 mL) was taken in a 0.5-cm quartz precision cell. Tetranitromethane was added from a microliter syringe (in 10-mL increments), and the solution was thoroughly mixed prior to each measurement. The concentration of TNM varied between 0.3 and 1.0 M. Since the absorption maxima of the EDA complexes were not apparent, the measurements were made at 480 and 500 nm, except for the haloanisoles, for which the measurements were made at 450 and 460 nm. Plots of [anisole]/A_{CT} against [TNM] were linear. Each plot consisted of at least eight data points, and the linear fit was obtained by the method of least squares with a correlation coefficient >0.99. The values of the extinction coefficient ϵ_{CT} and the formation constant K were evaluated from the intercept and slope according to eq 10.

Charge-Transfer Nitration of Anisoles. In a typical experiment a solution containing 0.1 M anisole and 0.83 M TNM in acetonitrile (5 mL) was irradiated with a focused beam from a 1000-W Hg–Xe lamp. The beam was passed through an IR water filter and a 425-nm cutoff filter. Irradiations were carried out in a Pyrex tube, immersed in cold water contained in a Pyrex dewar. As the reaction proceeded the solution changed from orange to either colorless or pale yellow. After photolysis, solvent and excess TNM were removed, and the crude product was dissolved in $CDCl_3$. Nitromethane (10 μL) was added as the internal standard and the ^1H NMR spectrum was recorded. The yield of the products was obtained from the integration of the methoxy resonances and the aromatic resonances as described in the individual cases. **Anisole**: Photonitration yielded a mixture of three compounds (81% overall yield) as indicated by methoxy resonances at δ 3.94, 3.91, and 3.84 in the ^1H NMR spectrum of the crude product. The products were identified as 2-nitro- (35%), 3-nitro- (3%), and 4-nitroanisole (43%) by GC and GC–MS analysis using commercially available authentic samples. **2-Methylanisole**: Photonitration yielded a mixture of two products as indicated by methoxy resonances at δ 3.94 and 3.88 in the ^1H NMR spectrum of the crude product. The combined yield of the two products was essentially quantitative. The products were identified as 2-methyl-4-nitroanisole (68%) and 2-methyl-6-nitroanisole (32%). The identifications were confirmed by GC analysis by the coinjection of authentic samples obtained in the thermal nitration of 2-methylanisole using fuming nitric acid. **3-Methylanisole**: The crude product obtained from the photolysis consisted of three products as indicated by methoxy resonances at δ 3.93, 3.87, and 3.82 in the ^1H NMR spectrum. GC analysis of the crude product also showed the presence of three products. The products were identified as 2-nitro (16%), 4-nitro (54%), and 6-nitro (30%) based on the GC analysis in comparison with commercially available authentic samples. The yields of the three products were based on the integration of the methoxy resonances in the ^1H NMR spectrum with nitromethane as the internal standard. **4-Fluoroanisole**: Photonitration yielded one major product, identified as 4-fluoro-2-nitroanisole, in 83% yield, from the ^1H NMR spectrum of the crude product. This identification was confirmed by GC analysis using authentic 4-fluoro-2-nitroanisole for coinjection. GC analysis also revealed the presence of a minor product, which was identified as 2,6-dinitro-4-fluorophenol from its ^1H NMR spectrum and GC–MS. **2,6-Dinitro-4-fluorophenol**: yield 14% (based on the integration of the doublet resonance at δ 8.12); ^1H NMR ($CDCl_3$) δ 8.12 (d, J_{H-F} = 7.08 Hz); MS (70 eV) m/z 202 (96, M^+), 125 (13), 111 (22), 110 (18), 109 (31), 98 (13), 97 (21), 82 (36), 81 (100), 80 (12), 73 (13), 70 (48), 69 (24), 63 (25). Nitroform, which was formed in the reaction, appeared as a singlet at δ 7.79 in the ^1H NMR spectrum of the crude product, and the yield was found to be quantitative from the integration of the singlet resonance. **4-Chloroanisole**: The ^1H NMR spectrum of the crude product indicated the formation of only 4-chloro-2-nitroanisole in quantitative yield. The product was identified by ^1H NMR spectral comparison and GC analysis with the authentic sample obtained from the thermal nitration of 4-chloroanisole.[65] A singlet at δ 7.82 in the ^1H NMR spectrum indicated the formation of nitroform, and integration of the peak showed the yield to be quantitative. **4-Bromoanisole**: The ^1H NMR spectrum of the crude product showed doublet resonances in the aromatic region at δ 8.18, 7.96, and 7.64 and methoxy resonances at δ 3.91, 3.95, and 3.87, corresponding to 4-nitroanisole (38%), 4-bromo-2-nitroanisole (42%), and 2,4-dibromoanisole (20%), respectively. A singlet resonance at δ 7.86 indicated the formation of nitroform in quantitative yield. The identity of the three aromatic products was confirmed by GC analysis by the coinjection of the corresponding authentic samples.

Charge-Transfer Trinitromethylation of Anisoles. Photolysis of charge-transfer complexes from various anisoles and TNM in dichloromethane was carried out as described in the charge-transfer nitration of anisoles. **Anisole**: A solution containing 0.1 M anisole and 0.83 M TNM in dichloromethane (5 mL) was photolyzed for 8 h. After removal of the solvent and excess TNM, the crude product was dissolved in acetone-d_6, and nitromethane (10 μL) was added. The ^1H NMR spectrum of the crude product indicated the presence of three major products with methoxy resonances at δ 3.95, 3.93, and 3.91. The presence of a pair of doublets in the aromatic region indicated 4-(trinitromethyl)anisole to be the major product. The integration of the aromatic doublet resonances indicated the yield of 4-(trinitromethyl)anisole to be ~40%. **4-(Trinitromethyl)anisole**: ^1H NMR (CD_3COCD_3) δ 7.75 (d, 2 H, H-3 and 5, J = 9.2 Hz), 7.22 (d, 2 H, H-2 and 6, J = 9.2 Hz), 3.95 (s, 3 H, OCH_3). The identity of 4-(trinitromethyl)anisole was confirmed by the hydrolysis of the trinitromethyl group[21] to yield 4-methoxybenzoic acid.

(67) Atherton, S. J. *J. Phys. Chem.* **1984**, *88*, 2840.
(68) Foyt, D. C. *J. Comput. Chem.* **1981**, *5*, 49.

The crude product was stirred with 5 mL of concentrated hydrochloric acid at room temperature for 12 h. The resulting mixture was extracted with methylene chloride. The extracts were combined and dried over anhydrous $MgSO_4$, and the solvent was removed to yield a reddish crystalline solid. Analysis of the crude product by ^1H NMR and GC–MS analysis indicated it to be a mixture of 4-methoxybenzoic acid, 2-nitroanisole, and 4-nitroanisole. **4-Methoxybenzoic acid**: ^1H NMR (CD_3COCD_3) δ 7.97 (d, 2 H, H-2 and 6, J = 9.0 Hz), 6.98 (d, 2 H, H-3 and 5, J = 9.0 Hz), 3.85 (s, 3 H, OCH_3); MS (70 eV) m/z 153 (19), 152 (71, M^+), 135 (100), 107 (15), 105 (18), 92 (21), 81 (11), 77 (40), 65 (12), 64 (20), 63 (28). The combined yield of 2-nitro- and 4-nitroanisole was 50%. 2-(Trinitromethyl)anisole was not formed in the reaction. **2-Methylanisole**: Irradiation of a solution containing 2-methylanisole (24 mg, 0.2 mmol) and TNM (392 mg, 2 mmol) in dichloromethane (3 mL) for 6 h resulted in the complete disappearance of 2-methylanisole. The ^1H NMR spectrum of the crude product indicated the presence of 2-methyl-4-(trinitromethyl)anisole as the major product. It was characterized after hydrolysis of the trinitromethyl group to yield 3-methyl-4-methoxybenzoic acid as described earlier.[69] 4-Nitro- and 6-nitro-2-methylanisole were obtained as minor products (16%) in the ratio 65/35, respectively. **3-Methylanisole**: A solution containing 0.1 M 3-methylanisole and 0.83 M TNM in dichloromethane (5 mL) was irradiated for 8 h. Removal of solvent and excess TNM yielded a reddish brown oil. It was dissolved in acetone-d_6, and then nitromethane (10 μL) was added as the internal standard. The ^1H NMR spectrum of the crude mixture showed the presence of one major product and three minor products. The major product was identified as 3-methyl-4-(trinitromethyl)anisole (62%): ^1H NMR (CD_3COCD_3) δ 7.19 (d, 1 H, J = 8.6 Hz), 7.00 (d, 1 H, J = 8.6 Hz), 7.10 (s, 1 H), 3.86 (s, 3 H, OCH_3), 2.48 (s, 3 H, 3-CH_3). The trinitromethyl group was hydrolyzed by treating the crude product with concentrated hydrochloric acid as described in the case of anisole to yield 2-methyl-4-methoxybenzoic acid, which was identified by ^1H NMR and GC–MS analysis: ^1H NMR (CD_3CN) δ 7.85 (d, 1 H, H-5, J = 8 Hz), 7.01 (s, 1 H, H-2), 6.92 (d, 1 H, H-6, J = 8 Hz), 3.98 (s, 3 H, OCH_3), 2.38 (s, 3 H, 2-CH_3); MS (70 eV) 166 (100, M^+), 149 (25), 137 (49), 133 (25), 121 (25), 119 (98), 106 (20), 93 (69), 91 (98), 78 (43), 77 (96), 65 (25). The three minor products were identified as 2-nitro-, 4-nitro-, and 6-nitro-3-methylanisole by GC analysis in comparison with the authentic samples. **4-Fluoroanisole**: A solution containing 4-fluoroanisole (0.5 mL, 4.4 mmol) and TNM (2 mL, 16.7 mmol) in dichloromethane (20 mL) was irradiated for 16 h. Removal of solvent and excess TNM yielded a yellow crystalline solid (0.92 g). The ^1H NMR spectrum of the crude product indicated methoxy resonances at δ 4.01, 3.95, and 3.83, corresponding to the formation of 2,6-dinitro-4-fluoroanisole (6%), 4-fluoro-2-nitroanisole (9%), and 4-fluoro-2-(trinitromethyl)anisole (72%). Recrystallization from a mixture of ether and hexane afforded 4-fluoro-2-(trinitromethyl)anisole as a yellow crystalline solid. **4-Fluoro-2-(trinitromethyl)anisole**: IR (KBr) 3098 (m), 2956 (m), 2878 (w), 2853 (m), 1631 (s), 1617 (s), 1598 (s), 1584 (s), 1498 (s), 1430 (m), 1359 (w), 1298 (s), 1277 (s), 1233 (s), 1177 (s), 1024 (s), 879 (m), 837 (s), 823 (s), 801 (s), 743 (s), 642 (m) cm^{-1}; ^1H NMR ($CDCl_3$) δ 7.44 (ddd, 1 H, H-5, J = 2.6, 7.0, 9.1 Hz), 7.09 (m, 2 H, H-3 and H-6), 3.83 (s, 3 H, OCH_3); ^{13}C NMR ($CDCl_3$) δ 161.7 (C-1), 153.1 (C-4, d, J_{C-F} = 100 Hz), 122.8 (C-5, d, J_{C-F} = 22 Hz), 116.8 (C-3, d, J_{C-F} = 28 Hz), 114.2 (C-6, d, J_{C-F} = 7.9 Hz), 56.9 (OCH_3). Anal. Calcd for $C_8H_6FN_3O_7$: C, 34.91; H, 2.18; N, 15.27. Found: C, 35.05; H, 2.22; N, 15.17. 4-Fluoro-2-nitroanisole was identified by ^1H NMR spectral comparison and GC analysis with the authentic sample. 2,6-Dinitro-4-fluoroanisole was identified by its ^1H NMR spectrum and GCMS: ^1H NMR ($CDCl_3$) δ 8.10 (d, J_{H-F} = 7.08 Hz), 4.01 (s, OCH_3); Ms (70 eV) m/z 217 (4, M^+), 202 (87), 139 (11), 125 (15), 111 (23), 110 (22), 109 (33), 98 (15), 97 (23), 86 (11), 83 (11), 82 (44), 81 (100), 80 (15), 70 (50), 69 (29), 63 (31), 62 (19). **4-Chloroanisole**: A solution containing 4-chloroanisole (0.5 mL, 4 mmol) and TNM (2 mL, 16.7 mmol) in dichloromethane (20 mL) was irradiated for 16 h. Removal of solvent and excess TNM yielded a yellow crystalline solid (0.83 g). The ^1H NMR spectrum of the crude product indicated the presence of 4-chloro-2-(trinitromethyl)anisole (67%) and 4-chloro-2-nitroanisole (7%). The major product was isolated as a yellow crystalline solid by recrystallization from a mixture of ether and hexane. **4-Chloro-2-(trinitromethyl)anisole**: IR (KBr) 3089 (w), 2956 (m), 2874 (w), 1629 (s), 1596 (s), 1491 (s), 1467 (w), 1408 (w), 1296 (s), 1275 (s), 1212 (m), 1146 (w), 1017 (s), 823 (s), 799 (s) cm^{-1}; ^1H NMR ($CDCl_3$) δ 7.67 (dd, 1 H, H-5, J = 2.4, 9.0 Hz), 7.29 (d, 1 H, H-3, J = 2.4 Hz), 7.06 (d, 1 H, H-6, J = 9.0 Hz), 3.84 (s, 3 H, OCH_3); ^{13}C NMR ($CDCl_3$) δ 157.6 (C-1), 135.9 and 129.3 (C-3 and C-5), 126.7 (C-4), 114.2 (C-6), 56.8 (OCH_3). Anal. Calcd for $C_8H_6ClN_3O_7$: C, 32.93; H, 2.06; N, 14.41. Found: C, 33.02; H, 2.09; N, 14.33. 4-Chloro-2-nitroanisole was identified by ^1H NMR spectral comparison with an authentic sample. **4-Bromoanisole**: A sample containing 4-bromoanisole (0.5 mL, 4 mmol) and TNM (2 mL, 16.7 mmol) in dichloromethane (20 mL) was irradiated for 16 h. Removal of solvent and excess TNM yielded a yellow crystalline solid (1.2 g). The ^1H NMR spectrum of the crude product showed methoxy resonances at δ 3.99, 3.94, 3.90, and 3.84, corresponding to 4-bromo-2-nitroanisole (7%), 4-nitroanisole (6%), 2,4-dibromoanisole (5%), and 4-bromo-2-(trinitromethyl)anisole (73%). The major product was isolated as a yellow crystalline solid by recrystallization from ether–hexane mixture. **4-Bromo-2-(trinitromethyl)anisole**: IR (KBr) 3085 (w), 2952 (m), 1629 (s), 1596 (s), 1488 (s), 1294 (s), 1273 (s), 1212 (m), 1017 (m), 820 (m), 799 (s) cm^{-1}; ^1H NMR ($CDCl_3$) δ 7.81 (dd, 1 H, H-5, J = 2.2, 8.9 Hz), 7.41 (d, 1 H, H-3, J = 2.2 Hz), 7.01 (d, 1 H, H-6, J = 8.8 Hz), 3.84 (s, 3 H, OCH_3); ^{13}C NMR ($CDCl_3$) δ 158.1 (C-1), 138.9 and 132.0 (C-3 and C-5), 114.5 (C-6), 113.4 (C-4), 56.8 (OCH_3). Anal. Calcd for $C_8H_6BrN_3O_7$: C, 28.58; H, 1.78; N, 12.5. Found: C, 28.67; H, 1.82; N, 12.42. The mother liquor was analyzed by GC and the presence of 4-bromo-2-nitroanisole, 4-nitroanisole, and 2,4-dibromoanisole was confirmed by coinjection of the corresponding authentic sample.

Photolysis of the EDA Complex from 4-Methylanisole and TNM in Various Solvents. General Procedure for Photolysis. In a typical experiment a 3-mL solution containing 4-methylanisole and excess TNM placed in a 1-cm quartz cell was irradiated with a focused beam from a 500-W Hg lamp. The beam passed through an IR water filter and 425-nm Pyrex cutoff filter. The solution was maintained at 25–30 °C by placing the cell in a Pyrex dewar containing cold water. The reaction was followed spectrophotometrically by the disappearance of the CT band. **CH_2Cl_2**: A solution containing 0.6 M 4-methylanisole and 0.66 M TNM was irradiated for 5 h. After removal of the solvent and excess TNM at the rotary evaporator, the mixture was dissolved in $CDCl_3$, and CH_3NO_2 (10 μL) was added as the internal standard. The ^1H NMR spectrum of the crude product indicated the formation of 4-methyl-2-(trinitromethyl)anisole (95%) and 4-methyl-2-nitroanisole (5%). The latter was identified by ^1H NMR spectral comparison and GC analysis with an authentic sample. A preparative-scale reaction was carried out by irradiating a solution containing 4-methylanisole (0.97 g, 8 mmol) and TNM (8.2 g, 42 mmol) in CH_2Cl_2 (10 mL) for 15 h. After removal of the solvent and excess TNM, the red-brown slurry was crystallized from a mixture of ether and hexane to yield 4-methyl-2-(trinitromethyl)anisole (1.5 g, 70%) as yellow crystals: mp 105–110 °C (decomposition with evolution of NO_2); IR (CH_2Cl_2) 1621 (s), 1590 (s), 1503 (m), 1421 (m), 1302 (m) cm^{-1}; ^1H NMR ($CDCl_3$) δ 7.49 (d, 1 H, H-5, J = 8.8 Hz), 7.05 (s, 1 H, H-3) 7.00 (d, 1 H, H-6, J = 8.8 Hz), 3.80 (s, 3 H, OCH_3), 2.35 (s, 3 H, 4-CH_3); ^{13}C NMR ($CDCl_3$) δ 157.0, 136.7, 131.1, 129.6, 112.7, 56.3, 20.5. (In all the 2-trinitromethyl derivatives obtained, C-2 and the trinitromethyl carbon could not be detected in the ^{13}C NMR spectrum, presumably due to ^{14}N-quadrupolar broadening and the absence of nuclear Overhauser enhancement.[38]) The identification of 4-methyl-2-(trinitromethyl)anisole was confirmed by the hydrolysis of the trinitromethyl group to yield 2-methoxy-5-methylbenzoic acid, as reported earlier.[69] **CH_2Cl_2 with Added TBAP**: A solution containing 0.6 M 4-methylanisole, 0.83 M TNM, and 0.2 M TBAP was irradiated for 5 h. Removal of solvent and excess TNM yielded a yellow crystalline solid. It was dissolved in $CDCl_3$, and CH_3NO_2 (10 μL) was added as the internal standard. The ^1H NMR spectrum of the crude product indicated the formation of 4-methyl-2-nitroanisole (65%) and 4-methyl-2-nitrophenol (35%). The identity of these two products was confirmed by GC analysis, by the coinjection of authentic samples. When the photolysis was repeated at 0 °C and the products were analyzed by ^1H NMR spectroscopy, a transient new species was detected: ^1H NMR ($CDCl_3$) δ 7.13 (d, 2 H, J = 10 Hz), 6.37 (d, 2 H, J = 10 Hz), 1.93 (s, 3 H, 4-CH_3). Upon leaving the sample at room temperature, the new species disappeared to yield 4-methyl-2-nitrophenol. The transient species was identified as 4-methyl-4-nitrocyclohexa-2,5-dienone, based on the ^1H NMR spectral comparison with that reported in the literature.[19]

In order to carry out the photolysis under strictly anhydrous conditions, the following experiment was performed. To a solution containing 0.06 M 4-methylanisole and 0.2 M TBAP in dry CH_2Cl_2 (5 mL), neutral alumina (~1 g, Woelm Pharma Super I grade) was added and the solution was stirred for 5 min under argon. TNM (0.5 mL) was added and the stirring was continued for an additional 2 min. The solution was photolyzed without stirring, after all the alumina settled. After 5 h the solution was filtered and the alumina was washed with CH_2Cl_2. The washings were combined with the filtrate and then the solvent was removed. Analysis of the crude product by GC indicated the formation of only 4-methyl-2-nitroanisole. The ^1H NMR spectrum of the crude product in $CDCl_3$ with CH_3NO_2 as the internal standard indicated formation of 4-methyl-2-nitroanisole (50%) and 4-methyl-2-(trinitro-

(69) Sankararaman, S.; Kochi, J. K. *Recl. Trav. Chim. Pays-Bas* **1986**, *105*, 278.

methyl)anisole (11%). **CH_2Cl_2 with Added TBAT**: A solution containing 0.06 M 4-methylanisole, 2.2 M TNM, and 0.01 M TBAT in CH_2Cl_2 (3 mL) was photolyzed for 6.5 h using a 500-nm Corning cutoff filter. After removal of the solvent and excess TNM, the crude product was obtained as a yellow solid. The ^1H NMR spectrum of the crude product indicated formation of 4-methyl-2-(trinitromethyl)anisole (76%) and 4-methyl-2-nitroanisole (24%). This was confirmed by GC analysis by the coinjection of authentic samples. **CH_3CN**: A solution containing 0.06 M 4-methylanisole and 1.67 M TNM in acetonitrile (3 mL) was irradiated for 6.5 h. After photolysis the solvent and excess TNM were removed, and the crude product was dissolved in $CDCl_3$. The ^1H NMR spectrum of the crude product revealed formation of 4-methyl-2-nitroanisole (66%), 4-methyl-2-nitrophenol (14%), and 2,6-dinitro-4-methylphenol (15%). The dinitrophenol was identified from its ^1H NMR spectrum, which showed singlets at δ 8.15 and 2.45 for the aromatic and the methyl protons, respectively. The mass spectrum of the dinitrophenol showed the molecular ion peak: MS (70 eV) m/z 198 (100, M^+), 140 (49), 107 (12), 105 (18), 78 (12), 77 (50), 76 (12), 66 (25), 65 (45), 63 (12), 53 (50). **CH_3CN with Added TBAP**: A solution containing 0.13 M 4-methylanisole, 1.39 M TNM, and 0.2 M TBAP in acetonitrile (3 mL) was irradiated for 6 h. After removal of the solvent and excess TNM, the crude product was obtained as a yellow solid. The ^1H NMR spectrum of the crude product indicated formation of 4-methyl-2-nitroanisole (56%), 4-methyl-2-nitrophenol (5%), and 2,6-dinitro-4-methylphenol (39%). The products were identified by GC and GC–MS analysis by coinjection of authentic samples. **CH_3CN with Added TBAT**: A solution containing 0.06 M 4-methylanisole, 1.39 M TNM, and 0.01 M TBAT was photolyzed for 7 h. After workup, the crude product contained 4-methyl-2-nitroanisole (77%), 4-methyl-2-nitrophenol (13%), and 4-methyl-2-(trinitromethyl)anisole ($\sim$10%). **Hexane**: Irradiation of a solution containing 0.06 M 4-methylanisole and 0.28 M TNM in hexane (3 mL) for 5 h resulted in the precipitation of the major product, which was identified as 4-methyl-2-(trinitromethyl)anisole (85%). 4-Methyl-2-nitroanisole was the minor product formed (15%). **Benzene**: Irradiation of a solution containing 0.03 M 4-methylanisole and 0.55 M TNM in benzene for 5 h yielded a mixture of 4-methyl-2-(trinitromethyl)anisole (85%) and 4-methyl-2-nitroanisole (15%), as determined from the ^1H NMR spectrum of the crude product. When the irradiation was performed in the presence of 0.01 M TBAP in benzene (3 mL) for 3.5 h, a mixture of 4-methyl-2-(trinitromethyl)anisole (75%) and 4-methyl-2-nitroanisole (25%) was obtained. Irradiation of a solution containing 0.06 M 4-methylanisole, 1.5 M TNM, and 0.01 M TBAT in benzene (3 mL) for 6.5 h using a 500-nm cutoff filter yielded 4-methyl-2-(trinitromethyl)anisole as the sole product (quantitative yield.)

Estimation of Nitrous Acid Formed during Charge-Transfer Alkylation of 4-Methylanisole. A solution containing 0.1 M 4-methylanisole (63 μL) and 0.83 M TNM (0.5 mL) in dichloromethane (5 mL) was irradiated with a focused beam from a 1000-W Hg–Xe lamp equipped with an IR water filter and a 425-nm Corning cutoff filter. The photolysis was carried at 0–5 °C (in an ice bath) for 5.5 h. Distilled water (2 mL) was added to the photolysate and then the entire mixture was transferred to a Schlenk tube. The side arm of the Schlenk tube was attached to a gas buret half-filled with oil. The lower end of the buret was attached to an oil reservoir. Initially the Schlenk tube and the gas buret were filled with argon. The system was allowed to attain equilibrium at room temperature (23 °C) for 30 min. A saturated aqueous solution of urea (2 mL) was introduced into the Schlenk tube using a hypodermic syringe, and the mixture was stirred vigorously for 45 min. The system was allowed to attain equilibrium before the final buret reading was taken. The volume of gas evolved in the reaction = (final buret reading) − (initial buret reading + 2 mL of urea solution). The volume of gas evolved at 23 °C was 7.0 mL. The amount of trinitromethylation product formed in the reaction was obtained from the ^1H NMR spectrum of the crude product as follows. The reaction mixture was extracted with CH_2Cl_2. The CH_2Cl_2 extracts were combined and dried over anhydrous $MgSO_4$. After the removal of the solvent the crude mixture was dissolved in $CDCl_3$, and nitromethane (10 μL) was added as the internal standard. The amount of 4-methyl-2-(trinitromethyl)anisole formed, obtained by the integration of the methoxy resonance at δ 3.82, was 0.21 mmol. Theoretically this corresponds to a total volume of 7.6 mL of gaseous products at 23 °C, from the reaction of 0.21 mmol of nitrous acid with excess urea according to the following stoichiometry.[11]

$$2HNO_2 + H_2NCONH_2 \rightarrow 2N_2 + CO_2 + 3H_2O$$

The experiment was repeated by irradiating a solution containing 0.16 M 4-methylanisole and 0.83 M TNM in benzene (5 mL) for 4.5 h. The volume of gas evolved at 23 °C was 11.6 mL (expected for 10.7 mL). The amount of trinitromethylation product formed was 0.33 mmol, as determined from the ^1H NMR spectrum of the crude product, using CH_3NO_2 as the internal standard.

The gaseous mixture was analyzed by GC–MS for N_2 and CO_2: MS (70 eV) m/z 44 (85, CO_2), 40 (62, argon), 32 (20), 30 (22), 28 (75, CO^+ and N_2), 16 (100, O), 14 (73, N).

Quantum Yield for Charge-Transfer Alkylation and Nitration. The quantum yields for the CT alkylation and nitration of 4-methylanisole were measured in various solvents and with added salts. The photolysis apparatus consisted of either a 500-W high-pressure mercury lamp or a 1000-W Hg–Xe lamp. A focused beam from the lamp was passed through an IR water filter, followed by a 520-nm interference filter (10-nm band-pass) used as a monochromator. Calibration of the lamp was performed with a Reinecke salt actinometer, as described by Wegner and Adamson.[24] The quantum yield of formation of 4-methyl-2-(trinitromethyl)anisole and 4-methyl-2-nitroanisole and the disappearance of 4-methylanisole were obtained from individual runs. In a typical experiment a 2-mL solution of 4-methylanisole and a (4–8)-fold excess of TNM was placed in a 1-cm quartz precision cell, which was irradiated for a given period of time. The absorbance of the solution at 520 nm was $\simeq$2.0 to ensure the complete absorption of the light. Conversions were kept to 10–15%. After photolysis, the photolysate was quantitatively analyzed by HPLC for 4-methyl-2-(trinitromethyl)anisole using a C-18 reverse-phase column and a mixture of methanol and water (80:20 vol %) as eluent. A calibration plot of the concentration of 4-methyl-2-(trinitromethyl)anisole against the integrated peak area was obtained by using a pure sample of 4-methyl-2-(trinitromethyl)anisole just prior to the HPLC analysis of the photolysates. Quantitative analysis for 4-methyl-2-nitroanisole was carried out by HPLC using a silica gel normal-phase column and a mixture of hexane and dichloromethane (80:20 vol %) as eluent. A calibration plot of the concentration of 4-methyl-2-nitroanisole against the integrated peak area was obtained by using an authentic sample prior to the HPLC analysis of the photolysates. The quantum yield for the disappearance of 4-methylanisole in various solvents was obtained by two different methods. 4-Methylanisole was quantitatively analyzed by HPLC by using a C-18 reverse-phase column and acetonitrile as the eluent before and after photolysis. Also the decrease in the absorption of the charge-transfer band at 520 nm was measured after 5-fold dilution of an aliquot of the solution with the appropriate solvent. Since TNM was present in large excess, the decrease in the absorption of the charge-transfer band was taken as a measure of the disappearance of 4-methylanisole. Within experimental error ($\pm$10%), the same value was obtained for the quantum yield of disappearance of 4-methylanisole using both the methods (Table IV).

Determination of the Deuterium Kinetic Isotope Effect for the CT Alkylation and Nitration of 4-Methylanisole. A solution containing 0.1 M 4-methylanisole (63 μL) and 0.83 M TNM (0.5 mL) in dichloromethane (5 mL) contained in a Pyrex tube was kept inside a Pyrex dewar containing water maintained at 25 °C. Irradiation of the stirred solution was performed with a focused beam from a 1000-W Hg–Xe lamp. The light was passed through an IR water filter and a Corning CS-3-72 (425 nm) glass cutoff filter. The disappearance of the charge-transfer band at 490, 520, and 550 nm was followed spectrophotometrically every 10 min. Since TNM was in large excess, pseudo-first-order kinetic treatment was used to fit the data using the equation $\log A = \log A_0 - kt$, where A is the absorbance of the charge-transfer band at time t and A_0 is the absorbance at $t = 0$ at a given wavelength. A plot of $\log A$ against time gave a linear fit, obtained by the method of least squares with a correlation coefficient of 0.997. The rate constant k_H was obtained from the slope of the linear plot. The value of the rate constant k_H obtained was 1.28×10^{-2} min^{-1} at all three monitoring wavelengths.

The procedure was repeated with 4-methylanisole-*2,6*-d_2 and the rate constant k_D for the disappearance of the charge-transfer band was similarly obtained. The value of k_D was 1.23×10^{-2} and 1.22×10^{-2} min^{-1} at 490 and 520 nm, respectively. Thus $k_H/k_D = (1.28 \times 10^{-2})/(1.23 \times 10^{-2}) = 1.04$ for the trinitromethylation of 4-methylanisole.

A solution containing a mixture of 0.05 M 4-methylanisole (31 μL) (MA) and 0.05 M 4-methylanisole-*2,6*-d_2 (MA-d_2) (32 μL) was prepared in 5 mL of acetonitrile. The relative amounts of the protio and the deuterio 4-methylanisoles in the mixture were determined by GC–MS analysis using the relative abundance of the molecular ion peaks (m/z = 122 and 124, respectively); i.e., Φ_{MA} = [abundance of m/z = 122]/[abundance of m/z = 124] = 97/100 = 0.97. An aliquot of TNM (0.5 mL, 4 mmol) was added to the mixture, and photolysis was carried out with a focused beam from a 1000-W Hg–Xe lamp equipped with an IR water filter and a 480-nm Corning (CS-3-71) cutoff filter. The disappearance of the charge-transfer band was monitored spectrophotometrically. At various conversions, a 1-mL aliquot of the photolysate was withdrawn. After the removal of solvent and excess TNM, the mixture was redissolved in acetonitrile and analyzed by GC–MS. The relative amounts of the unreacted MA and MA-d_2 were determined by using the relative abundance of the molecular ion peaks (m/z = 122 and 124, respectively); i.e., Φ_{MA} = [abundance of m/z = 122 after photolysis]/

Table XI. Kinetic Isotope Effect for Charge-Transfer Nitration[a]

time, min	conv, %	ratio of molecular ions (m/z) 122/124	167/168	153/154	NA/NP[b]
0	0	97/100			
10	4	82/100	67/68	97/100	1.32
25	10	93/100	57/54	96/100	1.27
55	20	93/100	58/61	90/100	1.50
145	41	100/71	58/58	100/96	1.56
		Φ^c_{MA} = 0.94	Φ^d_{NA} = 1.0	Φ^e_{NP} = 0.97	

[a] From CT irradiation of a solution of 0.05 M 4-methylanisole and 0.05 M 4-methylanisole-*2,6*-d_2 in 5 mL of acetonitrile containing 0.83 M TNM at $\lambda > 480$ nm. [b] NA = 4-methyl-2-nitroanisole; NP = 4-methyl-2-nitrophenol. [c] Average kinetic isotope effect for the disappearance of 4-methylanisole, excluding entries 2 and 5. [d] Average kinetic isotope effect for nitroanisole. [e] Average kinetic isotope effect for nitrophenol, excluding entry 3.

[abundance of m/z = 124 after photolysis]. The relative amounts of the products formed were also determined by GC-MS analysis using peaks m/z = 167 and 168 for 4-methyl-2-nitroanisole (NA) and 4-methyl-2-nitroanisole-*6*-d_1 (NA-d_1), respectively, i.e., Φ_{NA} = [abundance of m/z = 167]/[abundance of m/z = 168], and using peaks m/z = 153 and 154 for 4-methyl-2-nitrophenol (NP) and 4-methyl-2-nitrophenol-*6*-d_1 (NP-d_1), respectively, i.e., Φ_{NP} = [abundance of m/z = 153]/[abundance of m/z = 154]. The results obtained at various conversions are included in Table XI.

Spectral Evidence for Olefinic Intermediates in the CT Alkylation of Anisoles. A solution containing 0.06 M *p*-methylanisole and 0.28 M TNM in hexane (3 mL) was irradiated at 0 °C for 2 h with $\lambda > 425$ nm. The solvent and excess TNM were removed in vacuo at 0 °C, and the crude reaction mixture was dissolved in $CDCl_3$. The ^{1}H NMR spectrum of this solution contained the characteristic resonances of the unreacted starting material and 4-methyl-2-(trinitromethyl)anisole (vide supra). In addition, the ^{1}H NMR spectrum showed olefinic resonances as a multiplet occurring between 5 and 6.5 ppm and new methoxy and methyl resonances at 3.63 and 1.91 ppm, respectively. The integration of the methoxy and methyl resonances indicated the ratio of the olefinic intermediate to the alkylation product to be ~1:2.5. Attempts to isolate the olefinic intermediate were unsuccessful, since it decomposed at room temperature to give 4-methyl-2-(trinitromethyl)anisole. In the case of the 4-haloanisoles, the irradiation of the complexes in dichloromethane at 0 °C for a short duration was followed immediately by the ^{1}H NMR spectral analysis of the crude product. It indicated the presence of olefinic resonances and the corresponding methoxy and methyl resonances as minor components of the crude reaction mixture. Upon allowing the solutions to stand at room temperature, the olefinic resonances gradually disappeared and were replaced with those of the 4-halo-2-(trinitromethyl)anisoles. These unstable olefinic components could be the TNM adducts to the anisoles similar to the 1:1 adducts previously isolated with anthracene donors.[38]

Acknowledgment. We thank S. J. Atherton and M. A. J. Rodgers of the Center for Fast Kinetics Research (under support from NIH Grant RR00886 and The University of Texas, Austin) and the National Science Foundation and the Robert A. Welch Foundation for financial support.

Registry No. D_2, 7782-39-0; anisole, 100-66-3; 2-methylanisole, 578-58-5; 3-methylanisole, 100-84-5; 4-methylanisole, 104-93-8; 4-fluoroanisole, 459-60-9; 4-chloroanisole, 623-12-1; 4-bromoanisole, 104-92-7; 4-(trinitromethyl)anisole, 110175-17-2; 3-methyl-4-(trinitromethyl)anisole, 110175-18-3; 4-fluoro-2-(trinitromethyl)anisole, 110175-19-4; 4-chloro-2-(trinitromethyl)anisole, 110175-20-7; 4-bromo-2-(trinitromethyl)anisole, 110175-21-8; 4-methyl-2-(trinitromethyl)anisole, 108088-84-2.

Stabilization of Positive Charge by β Silicon

Joseph B. Lambert,*[1] Gen-tai Wang, Rodney B. Finzel, and Douglas H. Teramura

Contribution from the Department of Chemistry, Northwestern University, Evanston, Illinois 60201. *Received April 28, 1987*

Abstract: The largest acceleration by a trimethylsilyl group in the formation of β positive charge has been measured in *r*-4-*tert*-butyl-*c*-2-(trimethylsilyl)cyclohex-*t*-yl (**6**). As the trifluoroacetate, this molecule reacts 10^{12} times faster than cyclohexyl trifluoroacetate at 25 °C in 97% aqueous trifluoroethanol. Measurements for **6** were carried out on the 3,5-dinitrobenzoate, and the leaving group ratio was obtained from the closely related *cis*-2-(trimethylsilyl)cyclohexyl (**3**), for which the rates of both trifluoroacetate and 3,5-dinitrobenzoate could be measured. The trifluoroacetate of **3**, with a 60° disposition between the trimethylsilyl and leaving groups, reacted 7.2×10^7 more slowly than **6** with its 180° disposition of the analogous groups, but still 10^4 times faster than cyclohexyl. The rate ratios of both **3** and **6** were resolved into contributions from hyperconjugation and induction by analogy with the mathematics of β secondary deuterium isotope effects. In this way, it was determined that the antiperiplanar trimethylsilyl group causes an acceleration of 10^{10} from the hyperconjugative interaction and 10^2 from induction, and the skew geometry causes an acceleration of about 10^2 from hyperconjugation and 10^2 from induction.

Extrusion of the elements of R_3Si–X from a two-carbon fragment, in which X is a nucleofuge (eq 1), is a well-known and

$$R_3Si—CH_2—CH_2—X \rightarrow R_3Si—X + CH_2{=}CH_2 \quad (1)$$

well-studied procedure for generating a double bond.[2,3] The interesting role of silicon appears to parallel that of lone-pair-bearing or unsaturated substituents in anchimeric assistance. Scheme I depicts two mechanistic possibilities. In the upper portion, silicon serves as a true internal nucleophile, engaging in nonvertical participation, to form the siliconium (pentavalent) intermediate **1**. In the lower portion, silicon provides stabilization of the β positive charge without nuclear movement (vertical

Scheme I

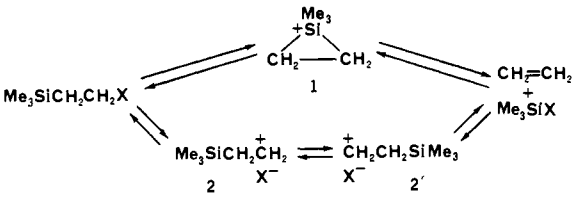

(1) Supported by the National Science Foundation (Grant No. CHE83-12285).

(2) Sommer, L. H.; Whitmore, F. C. *J. Am. Chem. Soc.* **1946**, *68*, 485-487.

(3) Chan, T.-H. *Acc. Chem. Res.* **1977**, *10*, 442-448.

0002-7863/87/1509-7838$01.50/0